environmental microbiology

Environmental Microbiology (2015) **17**(11), 4745–4763 doi:10.1111/1462-2920.13029

Cross-talk between a regulatory small RNA, cyclic-di-GMP signalling and flagellar regulator FlhDC for virulence and bacterial behaviours

Xiaochen Yuan,[1] Devanshi Khokhani,[1†] Xiaogang Wu,[1] Fenghuan Yang,[2] Gabriel Biener,[3] Benjamin J. Koestler,[4] Valerica Raicu,[1,3] Chenyang He,[2] Christopher M. Waters,[4] George W. Sundin,[5] Fang Tian[2] and Ching-Hong Yang[1*]**

[1]*Department of Biological Sciences, University of Wisconsin, Milwaukee, WI 53211, USA.*

[2]*State Key Laboratory for Biology of Plant Diseases and Insect Pests, Institute of Plant Protection, Chinese Academy of Agricultural Sciences, Beijing, 100193, China.*

[3]*Department of Physics, University of Wisconsin, Milwaukee, WI 53211, USA.*

[4]*Department of Microbiology and Molecular Genetics, Michigan State University, East Lansing, MI 48824, USA.*

[5]*Department of Plant, Soil, and Microbial Sciences, Michigan State University, East Lansing, MI 48824, USA.*

Summary

Dickeya dadantii **is a globally dispersed phytopathogen which causes diseases on a wide range of host plants. This pathogen utilizes the type III secretion system (T3SS) to suppress host defense responses, and secretes pectate lyase (Pel) to degrade the plant cell wall. Although the regulatory small RNA (sRNA) RsmB, cyclic diguanylate monophosphate (c-di-GMP) and flagellar regulator have been reported to affect the regulation of these two virulence factors or multiple cell behaviours such as motility and biofilm formation, the linkage between these regulatory components that coordinate the cell behaviours remain unclear. Here, we revealed a sophisticated regulatory network that connects the sRNA, c-di-GMP signalling and flagellar master regulator FlhDC. We propose multi-tiered regulatory mechanisms that link the FlhDC to the T3SS through three distinct pathways including the FlhDC-FliA-$YcgR_{3937}$ pathway; the FlhDC-EcpC-RpoN-HrpL pathway; and the FlhDC-*rsmB*-RsmA-HrpL pathway. Among these, EcpC is the most dominant factor for FlhDC to positively regulate T3SS expression.**

Received 5 June, 2015; revised 14 August, 2015; accepted 15 August, 2015. For correspondence. *E-mail chyang@uwm.edu; Tel. 414-229-6331; Fax 414-229-3926. **E-mail ftian@ippcaas.cn; Tel. +86-10-62896063; Fax +86-10-62894642. †Current address for D. Khokhani: Department of Plant Pathology, University of Wisconsin-Madison, Madison, WI 53706, USA.

Introduction

Dickeya dadantii 3937, belonging to the *Enterobacteriaceae* family, is a Gram-negative plant pathogen that causes soft rot, wilt and blight diseases on a wide range of plant species, including many economically important vegetables such as potato, tomato and chicory (Czajkowski *et al*., 2011). Many virulence factors contribute to the pathogenesis of *D. dadantii* at different stages of infection. For example, during the primary stage of infection, *D. dadantii* produces several factors that enhance its adhesion to the plant surface, such as cellulose fibrils, CdiA-type V secreted proteins and a biosurfactant (Rojas *et al*., 2002; Hommais *et al*., 2008; Jahn *et al*., 2011; Prigent-Combaret *et al*., 2012). Chemotaxis and motility are essential when *D. dadantii* needs a favourable site to enter into the plant apoplast (Antúnez-Lamas *et al*., 2009). In the apoplast, *D. dadantii* uses a type III secretion system (T3SS) to further invade the plant host (Bauer *et al*., 1994; Yang *et al*., 2002) by translocating virulence effector proteins into the host cytoplasm, thereby causing disease symptoms (Hueck, 1998; He *et al*., 2004; Mota *et al*., 2005). At later stage of infection, large areas of maceration on plant leaves and tissues occur due to the production and secretion of plant-cell-wall degrading enzymes, such as pectate lyases, proteases, cellulases and polygalacturonases (Collmer and Keen, 1986; Roy *et al*., 1999; Herron *et al*., 2000; Kazemi-Pour *et al*., 2004).

The T3SS of *D. dadantii* is encoded by a group I *hrp* gene cluster, in which the alternative sigma factor HrpL is required to activate most *hrp* operons (Alfano and Collmer, 1997). Two regulatory pathways to control the expression of *hrpL* have been discovered in *D. dadantii* (Yap *et al*., 2005; Tang *et al*., 2006; Yang *et al*., 2008a,b). The first pathway is through the two-component signal

© 2015 Society for Applied Microbiology and John Wiley & Sons Ltd

transduction system (TCS) HrpX/HrpY, which directly activates *hrpS* transcription. HrpS is a σ^{54} (RpoN)-enhancer binding protein, that binds a σ^{54}-containing RNA polymerase holoenzyme and initiates the transcription of *hrpL* (Chatterjee *et al*., 2002; Yap *et al*., 2005; Tang *et al*., 2006). Hence, HrpL is able to activate most genes downstream in the T3SS regulatory cascade, such as *hrpA*, *hrpN* and *dspE*, which encode the T3SS pilus protein, a harpin protein and a virulence effector respectively (Wei and Beer, 1995; Chatterjee *et al*., 2002; Tang *et al*., 2006). *hrpL* is also post-transcriptionally regulated by the RsmA/*rsmB* RNA-mediated pathway (Chatterjee *et al*., 2002; Yang *et al*., 2008b). RsmA is a small RNA-binding protein that binds to the 5′ untranslated region of *hrpL* mRNA, and facilitates its degradation (Chatterjee *et al*., 1995). RsmB is an untranslated regulatory RNA that binds to RsmA and sequesters its negative effect on *hrpL* messenger (m)RNA (Liu *et al*., 1998; Chatterjee *et al*., 2002). The global two-component system GacS/A upregulates RsmB RNA production, which alternatively increases downstream T3SS gene expression (Yang *et al*., 2008b). How these regulatory pathways are coordinated to regulate T3SS gene expression remains unclear.

Recent work from our laboratory demonstrated that a bacterial second messenger bis-(3′-5′)-cyclic dimeric guanosine monophosphate (c-di-GMP) is a global regulatory signal in *D. dadantii* controlling the expression of T3SS-encoding genes, the production of pectate lyase, swimming and swarming motility and biofilm formation (Yi *et al*., 2010). This is in agreement with the function of c-di-GMP in many other bacterial species showing that c-di-GMP regulates diverse cellular activities (Cotter and Stibitz, 2007; Hengge, 2009; Schirmer and Jenal, 2009; Römling, 2012). The synthesis and degradation of c-di-GMP are controlled by two types of enzymes performing opposing activities. They are the GGDEF domain-containing diguanylate cyclases (DGC) which convert two molecules of guanosine-5′-triphosphate (GTP) to cyclic diguanylate monophosphate (c-di-GMP) (Paul *et al*., 2004; Solano *et al*., 2009) and the EAL or the HD-GYP domain-containing phosphodiesterases (PDE), which break down c-di-GMP into 5′-phosphoguanylyl-(3′-5′)-guanosine (pGpG) or two guanosine monophosphates respectively (Schmidt *et al*., 2005; Tamayo *et al*., 2005; Ryan *et al*., 2006). In order for c-di-GMP to exert such diverse influences in the cell, a range of cellular c-di-GMP effectors have been identified including PilZ domain proteins, transcription factors, enzymatically inactive GGDEF and/or EAL domain proteins and RNA riboswitches. These effectors are able to directly interact with c-di-GMP which either activates or represses their activity (Hengge, 2009; Breaker, 2011; Ryan *et al*., 2012).

It has long been established that flagellar gene expression and assembly is a highly regulated process and occurs in a hierarchical manner. In *Escherichia coli* and other enteric bacteria, FlhDC is the master regulator, also defined as class I operon in flagellar assembly genes (Wang *et al*., 2006). FlhDC activates the expression of class II operons which encode the basal body and hook of the flagellum and an alternative σ factor (σ^{28}) FliA. FliA is required for the activation of class III operons which encode proteins for the outer subunits of the flagellum, chemotaxis and the flagellar motor (Chilcott and Hughes, 2000; Aldridge *et al*., 2006). Recently, it has been reported that FlhDC regulates the expression of genes encoding GGDEF domains in *E. coli* (Pesavento *et al*., 2008). In addition, FlhDC positively regulates the gene expression of T3SS and the extracellular enzyme production in *Pectobacterium carotovorum* by activating the expression of *rsmB* regulatory RNA (Cui *et al*., 2008). The homologue of FlhDC was also found in the genome of *D. dadantii* 3937, but its regulatory function has not been fully characterized yet.

C-di-GMP control of flagellar motility has been well studied in some bacterial species (Ryjenkov *et al*., 2006; Hengge, 2009). For example, the PilZ-domain protein YcgR slows down flagellar rotation by directly binding to switch complex proteins under elevated c-di-GMP conditions (Fang and Gomelsky, 2010; Paul *et al*., 2010). C-di-GMP also directly controls motility by transcriptional regulation of flagellar synthesis in *Vibrio cholerae* (Srivastava *et al*., 2013) and indirectly though induction of extracellular polysaccharides which inhibit motility via undescribed mechanisms in *V. cholerae* and *Salmonella* (Srivastava *et al*., 2013; Zorraquino *et al*., 2013).

In this study, we further investigated the impact of the PDEs EGcpB and EcpC on c-di-GMP-regulated behaviours in *D. dadantii* 3937. We identified two PilZ domain proteins $YcgR_{3937}$ and $BcsA_{3937}$, and determined their roles and functional relationship with EGcpB and EcpC. Then we systematically investigated the multi-tiered regulatory pathways linking the flagellar master regulator FlhDC to c-di-GMP signalling and T3SS gene expression. We found that EcpC is the major contributor that controls the T3SS through FlhDC.

Results

Elevated c-di-GMP levels were detected in D. dadantii *Δ*egcpB*, Δ*ecpC *and Δ*egcpB*Δ*ecpC

Previously, we identified two PDE-encoding genes *egcpB* (former name was *ecpB*), and *ecpC* in *D. dadantii* (Yi *et al*., 2010). Deletion of these PDE-encoding genes resulted in increased biofilm formation and reduced swimming motility, pectate lyase production, T3SS gene expression and overall virulence, suggesting that the c-di-GMP level in these mutants is increased compared with the wild-type strain (Yi *et al*., 2010). To determine if

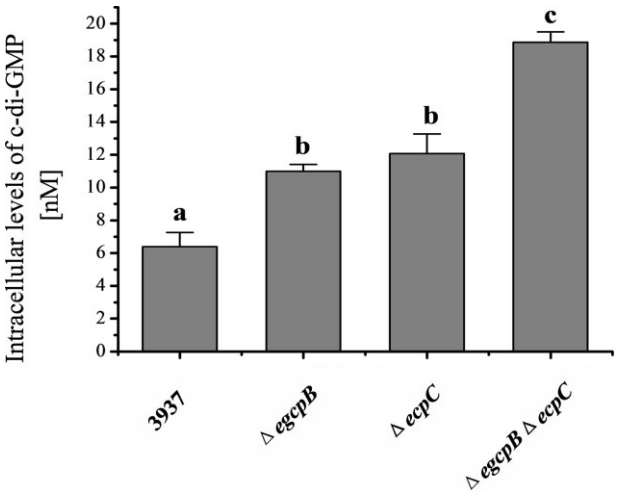

Fig. 1. Measurement of intracellular levels of c-di-GMP in wild-type *Dickeya dadantii*, Δ*egcpB*, Δ*ecpC* and Δ*egcpB*Δ*ecpC*. Assays were performed as described in the Experimental procedures. Error bars indicate standard errors of the means. Different lowercase letters above the bar indicate statistically significant differences between treatments ($P < 0.05$ by Student's *t*-test).

these phenotypes observed in the above PDE mutants were indeed due to elevated c-di-GMP levels, we performed liquid chromatography-mass spectrometry to measure the intracellular c-di-GMP concentration in the wild-type and in the PDE mutants. As expected, our results showed an increased c-di-GMP concentration in Δ*egcpB*, Δ*ecpC* and Δ*egcpB*Δ*ecpC* in comparison with the wild-type strain (Fig. 1), suggesting that the two PDEs EGcpB and EcpC indeed reduce c-di-GMP concentration in *D. dadantii* 3937. The fact that the double-deletion mutant had the highest level of c-di-GMP indicated that the effect of EGcpB and EcpC was not completely redundant, which is consistent with the previous report that Δ*egcpB*Δ*ecpC* showed more drastic changes phenotypically than either Δ*egcpB* or Δ*ecpC* (Yi *et al*., 2010).

PilZ domain proteins regulated biofilm formation, swimming motility and pectate lyase production in D. dadantii *under elevated c-di-GMP conditions*

C-di-GMP effectors are responsible for directly sensing intracellular changes in c-di-GMP levels and regulating cellular activity. PilZ domain proteins are the most widely distributed c-di-GMP effectors in bacteria (Hengge, 2009). After searching the genome of *D. dadantii* 3937 genome using the PFAM program, we found two genes, $ycgR_{3937}$ (ABF-0014564) and $bcsA_{3937}$ (ABF-0017612), encoding PilZ domains (Fig. 2). Domain structure analysis using the simplified modular architecture research tool (SMART) revealed that $YcgR_{3937}$, similar to the *E. coli* YcgR protein, has an N-terminal YcgR domain and a C-terminal PliZ domain, and $BcsA_{3937}$ is an *E. coli* BcsA-like protein, which has an N-terminal cellulose synthesis domain and a C-terminal PilZ domain (Fig. 2A). Amino acid sequence alignments of the reported PilZ domains from *E. coli* and those identified in *D. dadantii* 3937 suggested that the c-di-GMP binding motif (RxxxR) is conserved in the PilZ domain of both $YcgR_{3937}$ and $BcsA_{3937}$ proteins (Fig. 2B).

To investigate whether the regulatory pathway of EGcpB and EcpC was mediated by the two PilZ domain proteins, we constructed $ycgR_{3937}$ and $bcsA_{3937}$ gene deletion mutants in the wild type, Δ*egcpB* and Δ*ecpC* backgrounds, and examined biofilm formation, swimming motility and pectate lyase production in these mutants. As shown in Fig. 3, compared with the wild type, there was no detectable impact on biofilm formation, swimming motility or pectate lyase production when $bcsA_{3937}$ and $ycgR_{3937}$ were deleted in the wild-type background (Fig. 3). This is in agreement with earlier results demonstrating that increased c-di-GMP level is required for triggering the activity of PilZ-domain proteins (Paul *et al*., 2010). Compared with Δ*egcpB* and Δ*ecpC*, no further changes in swimming motility were detected when $bcsA_{3937}$ was deleted in these backgrounds (Fig. 3A). However, both $\Delta bcsA_{3937}$Δ*egcpB* and $\Delta bcsA_{3937}$Δ*ecpC*

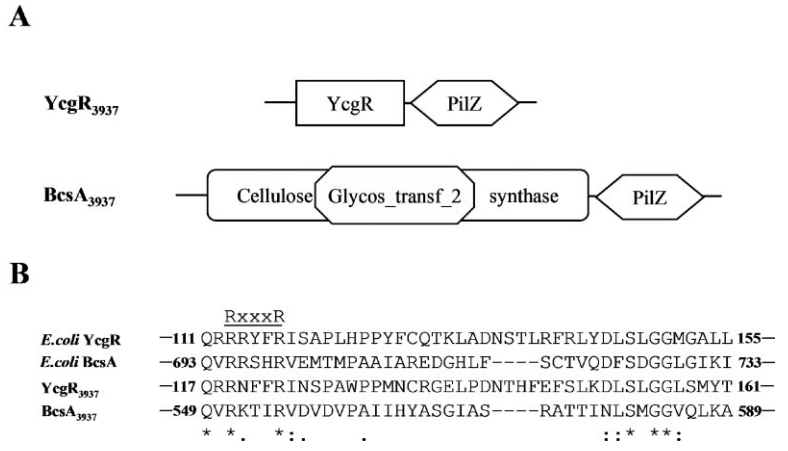

Fig. 2. Analysis of PilZ-domain proteins.
A. PilZ-domain proteins $YcgR_{3937}$ and $BcsA_{3937}$ in *Dickeya dadantii* 3937. Protein domains were predicted by the simplified modular architecture research tool (SMART).
B. Amino acid sequence alignment for the PilZ domains in *E. coli* and *D. dadantii*. c-di-GMP binding motif RxxxR is marked. '*' means that the residues are identical in all sequences in the alignment, ':' means that conserved substitutions have been observed, '.' Means that semi-conserved substitutions are observed.

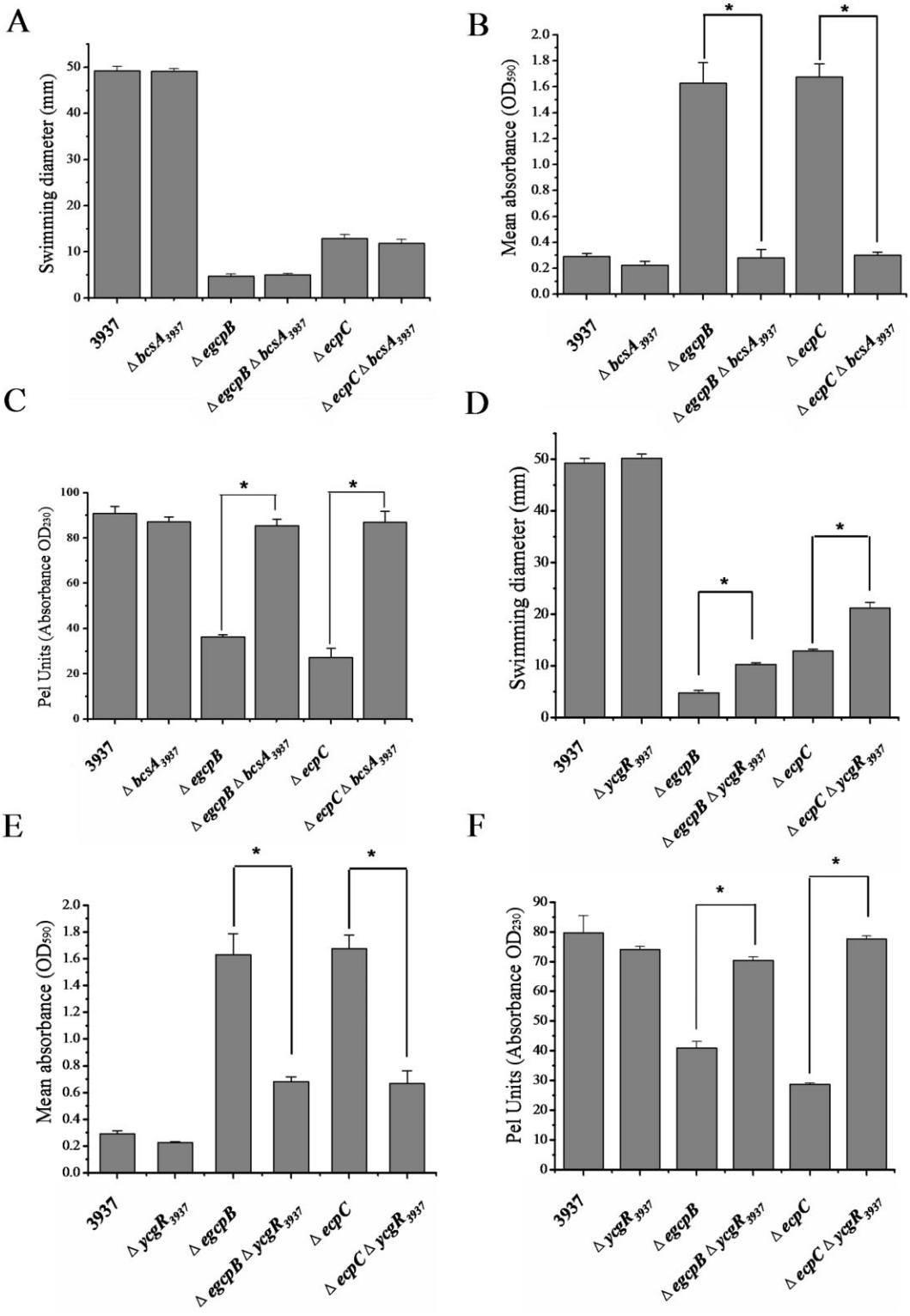

Fig. 3. The impact of mutation of $bcsA_{3937}$ and $ycgR_{3937}$ on various virulence phenotypes were examined. Bacterial swimming motility (A), biofilm formation (B) and pectate lyase production (C) were measured in the parental strain *D. dadantii* 3937, Δ$bcsA_{3937}$, Δ*egcpB*, Δ*egcpB*Δ$bcsA_{3937}$, Δ*ecpC* and Δ*ecpC*Δ$bcsA_{3937}$ respectively. The same assays were also tested in the parental strain 3937, Δ$ycgR_{3937}$, Δ*egcpB*, Δ*egcpB*Δ$ycgR_{3937}$, Δ*ecpC* and Δ*ecpC*Δ$ycgR_{3937}$ (D–F). Assays were performed as described in *Experimental procedures*. The experiments were repeated three independent times with similar results. The figure represents results from one experiment which includes three to five technical replicates. Error bars indicate standard errors of the means. Asterisks indicate statistically significant differences of the means ($P < 0.05$ by Student's *t*-test).

were fully restored to wild-type levels in biofilm formation (Fig. 3B). A full restoration of pectate lyase production was also observed when *bcsA*$_{3937}$ was deleted in either the Δ*egcpB* and Δ*ecpC* backgrounds (Fig. 3C). Moreover, deletion of *ycgR*$_{3937}$ in the Δ*egcpB* and Δ*ecpC* backgrounds led to partial restoration of swimming motility and biofilm formation, and full restoration of pectate lyase production (Fig. 3D–F).

To conclude, we propose that PilZ domain proteins BcsA$_{3937}$ and YcgR$_{3937}$ participate in the regulation of biofilm formation and pectate lyase production at elevated levels of c-di-GMP in *D. dadantii* 3937. In addition, YcgR$_{3937}$ but not BcsA$_{3937}$ regulates swimming motility when the intracellular levels of c-di-GMP are elevated.

YcgR$_{3937}$ *and BcsA*$_{3937}$ *differentially regulated T3SS gene expression under elevated c-di-GMP conditions*

Next, we wanted to determine whether YcgR$_{3937}$ and BcsA$_{3937}$ mediated regulation of T3SS gene expression, since EGcpB and EcpC affected T3SS gene expression in *D. dadantii* 3937 (Yi *et al*., 2010). The promoter activity of the *hrpA* gene, which encodes the T3SS pilus protein, was measured in wild-type and mutant strains. As expected, deleting the *ycgR*$_{3937}$ and *bcsA*$_{3937}$ gene in the wild-type background did not affect *hrpA* promoter activity. Interestingly, a further reduction of *hrpA* expression was observed in Δ*bcsA*$_{3937}$Δ*egcpB* and Δ*bcsA*$_{3937}$Δ*ecpC* compared with the Δ*egcpB* and Δ*ecpC* backgrounds, respectively (Fig. 4A), suggesting that BcsA$_{3937}$ might regulate T3SS gene expression in parallel with EGcpB and EcpC. In contrast, the Δ*egcpB*Δ*ycgR*$_{3937}$ mutant partially restored *hrpA* promoter activity to the wild-type level compared with the *egcpB* single mutant (Fig. 4B). But there was no detectable impact on T3SS gene expression when *ycgR*$_{3937}$ was deleted in the Δ*ecpC* background (Fig. 4B). Thus, we concluded that EGcpB, but not EcpC, affected T3SS gene expression through YcgR$_{3937}$.

Binding of YcgR$_{3937}$ *to c-di-GMP is required for regulating T3SS gene expression*

Since the above results demonstrated that YcgR$_{3937}$ was in the signalling pathway of EGcpB to regulate the T3SS, we were interested in determining whether this regulation was related to its binding to c-di-GMP. First, we examined whether YcgR$_{3937}$ bound c-di-GMP *in vivo* and *in vitro*. The results from isothermal tritration colorimetry (ITC) assay revealed that the purified YcgR$_{3937}$ protein was capable of binding c-di-GMP at a 1:1 stoichiometric ratio with an estimated dissociation constant (K_d) of 413 ± 64 nM (Fig. S1A). In contrast, the YcgR$_{3937}^{R124D}$ protein failed to bind c-di-GMP due to the mutation of the second arginine in the RxxxR motif in YcgR$_{3937}$, which is agreement with

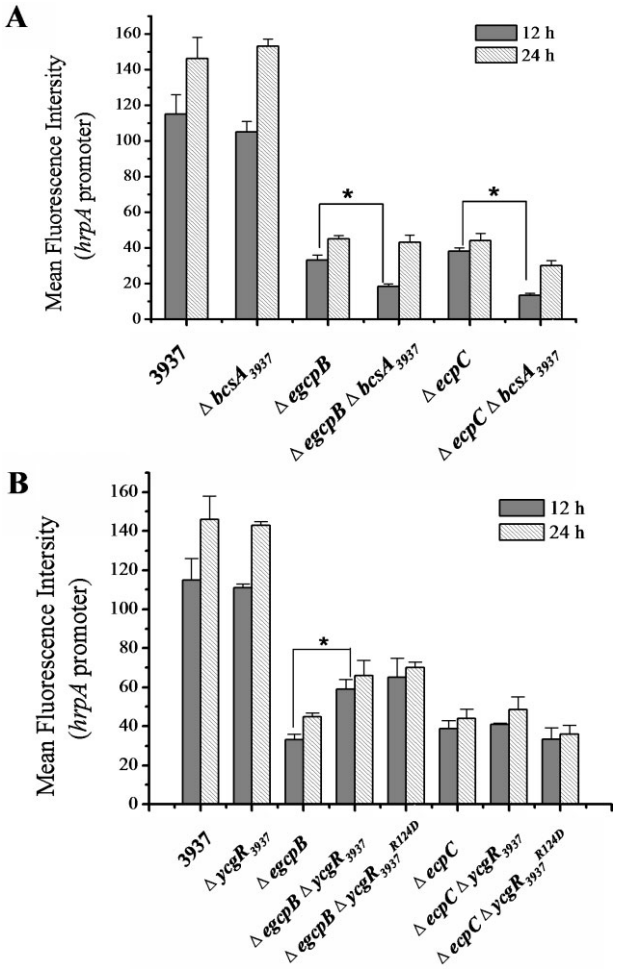

Fig. 4. The impact of mutation of *bcsA*$_{3937}$ and *ycgR*$_{3937}$ on *hrpA* promoter activity was examined. (A) The *hrpA* promoter activity was measured in the parental strain *D. dadantii* 3937, Δ*bcsA*$_{3937}$, Δ*egcpB*, Δ*egcpB*Δ*bcsA*$_{3937}$, Δ*ecpC* and Δ*ecpC*Δ*bcsA*$_{3937}$ respectively. Cells cultured under T3SS-inducing condition were used to measure the mean fluorescence intensity (MFI) by flow cytometry. The same assays were performed in the parental strain 3937, Δ*ycgR*$_{3937}$, Δ*egcpB*, Δ*egcpB*Δ*ycgR*$_{3937}$, Δ*egcpB ycgR*$_{3937}^{R124D}$, Δ*ecpC*, Δ*ecpC*Δ*ycgR*$_{3937}$ and Δ*ecpC ycgR*$_{3937}^{R124D}$ (B). The experiments were repeated three independent times with similar results. The figure represents results from one experiment which includes three technical replicates. Error bars indicate standard errors of the means. Asterisks indicate statistically significant differences of the means ($P < 0.05$ by Student's *t*-test).

the notion that these arginine residues are critical for the recognition of c-di-GMP by PilZ domains (Ryjenkov *et al*., 2006) (Fig. S1B). To probe the interaction between YcgR$_{3937}$ and c-di-GMP in living cells, we constructed a biosensor, in which YcgR$_{3937}$ was fused to yellow (YFP) and cyan (CFP) fluorescent proteins at the N- and C-terminus respectively. The CFP and YFP acted as a donor–acceptor pair in a process of Förster resonance energy transfer (FRET), which relies on the distance-dependent transfer of energy from an excited donor fluorescent protein to an acceptor fluorescent protein (Raicu

Table 1. Mean ± SEM (standard errors of the mean) of apparent FRET efficiency for wild-type and Δ*egcpB*Δ*ecpC* cells expressing the c-di-GMP sensor YFP-YcgR$_{3937}$-CFP.

Sample	12 hrs/0 μM	12 hrs/50 μM	12 hrs/100 μM	24 hrs/50 μM
Wild type	0.253 ± 0.002 (n = 10)	0.310 ± 0.002 (n = 11)	0.363 ± 0.001 (n = 5)	0.402 ± 0.003 (n = 10)
Δ*egcpB*Δ*ecpC* mutant	0.257 ± 0.003 (n = 10)	0.291 ± 0.002 (n = 10)	0.339 ± 0.004 (n = 5)	0.405 ± 0.002 (n = 10)

Various induction levels were tested (listed as 'time μM^{-1}' IPTG in the table) to establish the dynamic range of the sensor. The sensor was sensitive to changes in the concentrations of c-di-GMP when it was incubated for approximately 12 h with 50 to 100 μM IPTG. An order-of-magnitude estimate of the sensor concentration based on the intensity of donor emission corrected for FRET, F^D (Patowary *et al*., 2013), as described in the Experimental procedures section, suggested that the sensor expression level varied between roughly 10 molecules per cell, for 12 h incubation with 0 μM IPTG (first column), and 1000 sensor molecules per cell, for 24 h incubation with 50 μM IPTG (fourth column). The sensor concentration around which the sensor responded to changes in c-di-GMP concentrations, shown in the second and third columns in the Table, were on the order of 100 sensor molecules per cell. Within that concentration range, significant differences between the FRET efficiencies of the wild type and Δ*egcpB*Δ*ecpC* mutant were observed. n = number of FRET images. FRET images contained an average of 50 cells per image.

and Singh, 2013). Previous studies using a biosensor derived from *Salmonella enterica* serovar Typhimurium protein YcgR (YFP-YcgR-CFP) in diverse Gram-negative bacterial species demonstrated that the YcgR-based c-di-GMP sensor undergoes a conformational change that pushes the donor and acceptor apart when c-di-GMP binds to the PilZ domain of YcgR; this leads to reduction in the overall FRET efficiency of the cell, which is inversely proportional to the concentration of c-di-GMP (Benach *et al*., 2007; Christen *et al*., 2007; 2010; Kulasekara *et al*., 2013). As shown in Table 1 (second and third columns), significant differences between the FRET efficiencies of the wild-type and Δ*egcpB*Δ*ecpC* strains were observed, which were consistent with the result from mass spectrometry assay showing higher concentrations of c-di-GMP for the Δ*egcpB*Δ*ecpC* strain than the wild type (Fig. 1). To conclude, these results strongly indicate that YcgR$_{3937}$ directly interacts with c-di-GMP in *D. dadantii* 3937.

Next, we performed a chromosomal replacement of *ycgR*$_{3937}$ with *ycgR*$_{3937}^{R124D}$ in Δ*egcpB* background, and checked the T3SS gene expression in this strain. As shown in Fig. 4B, the promoter activity of the *hrpA* gene was recovered to a level similar to that in the Δ*egcpB*Δ*ycgR*$_{3937}$ double mutant. Based on these results, we propose that YcgR$_{3937}$ negatively regulates T3SS gene expression only under high c-di-GMP condition in the Δ*egcpB* background, and that this activity is triggered by directly sensing the intracellular c-di-GMP concentration via the YcgR$_{3937}$ PilZ domain. Similar experiments were also carried out in the Δ*ecpC* background. No further change in *hrpA* gene expression was detected (Fig. 4B), which was consistent with the above data showing that YcgR$_{3937}$ did not mediate the T3SS gene expression regulation via EcpC.

In a study by Tuckerman and colleagues, an *E. coli* protein complex, termed 'degradosome' contained a DGC and PDE which mediate the c-di-GMP-dependent RNA processing (Tuckerman *et al*., 2011). We used a bacterial adenylate cyclase two-hybrid (BACTH) system to test whether there is a physical interaction between YcgR$_{3937}$ and EGcpB or EcpC in *D. dadantii*. No positive signal was detected using different protein combinations, suggesting that neither EGcpB nor EcpC directly interacts with YcgR$_{3937}$ (data not shown).

The flagellar master regulator FlhDC positively controls the expression of the T3SS regulon in D. dadantii

Studies that compare the flagellum and the T3SS in several bacterial species demonstrated a close link between these two nanomachines in terms of structure, function and expression regulation (Young *et al*., 1999; Lee and Galán, 2004; Pallen *et al*., 2005; Erhardt *et al*., 2010). In enteric bacteria such as *E. coli* and *Salmonella*, the flagellar gene regulon has a three-tier hierarchy, which is controlled by class I master regulator FlhDC, and class II alternative sigma factor FliA (Macnab, 1996). FliA is required for the activation of all flagellar class III genes that encode the structural components of the flagellum (Liu and Matsumura, 1994). Homologues of both FlhDC and FliA are present in *D. dadantii*. Deletion of *flhDC* or *fliA* led to significantly reduced motility, indicating that they are important regulators for motility in *D. dadantii* (Fig. S2). To determine whether there is a similar gene expression hierarchy in *D. dadantii*, we examined the promoter activity of *fliA* in wild-type and Δ*flhDC* strains. The results showed that the promoter activity of *fliA* was reduced dramatically in the Δ*flhDC* mutant, and was restored to the wild-type level in the complemented strain (Fig. 5A), suggesting that FlhDC strictly controls the expression of *fliA*.

In *P. carotovorum*, Cui and colleagues (2008) discovered that the expression of T3SS *hrp* regulon is controlled by FlhDC. Therefore, we asked whether the homologues of FlhDC and FliA in *D. dadantii* regulate the T3SS. To test this, we first examined the promoter activity of *hrpL*, *hrpA* and *hrpN* in the wild-type, Δ*flhDC* and Δ*fliA* strains. Deletion of *flhDC* significantly decreased both the promoter activity of *hrpA* (3.9-fold), *hrpN* (6.6-fold) and *hrpL* (1.9-fold) under T3SS-inducing

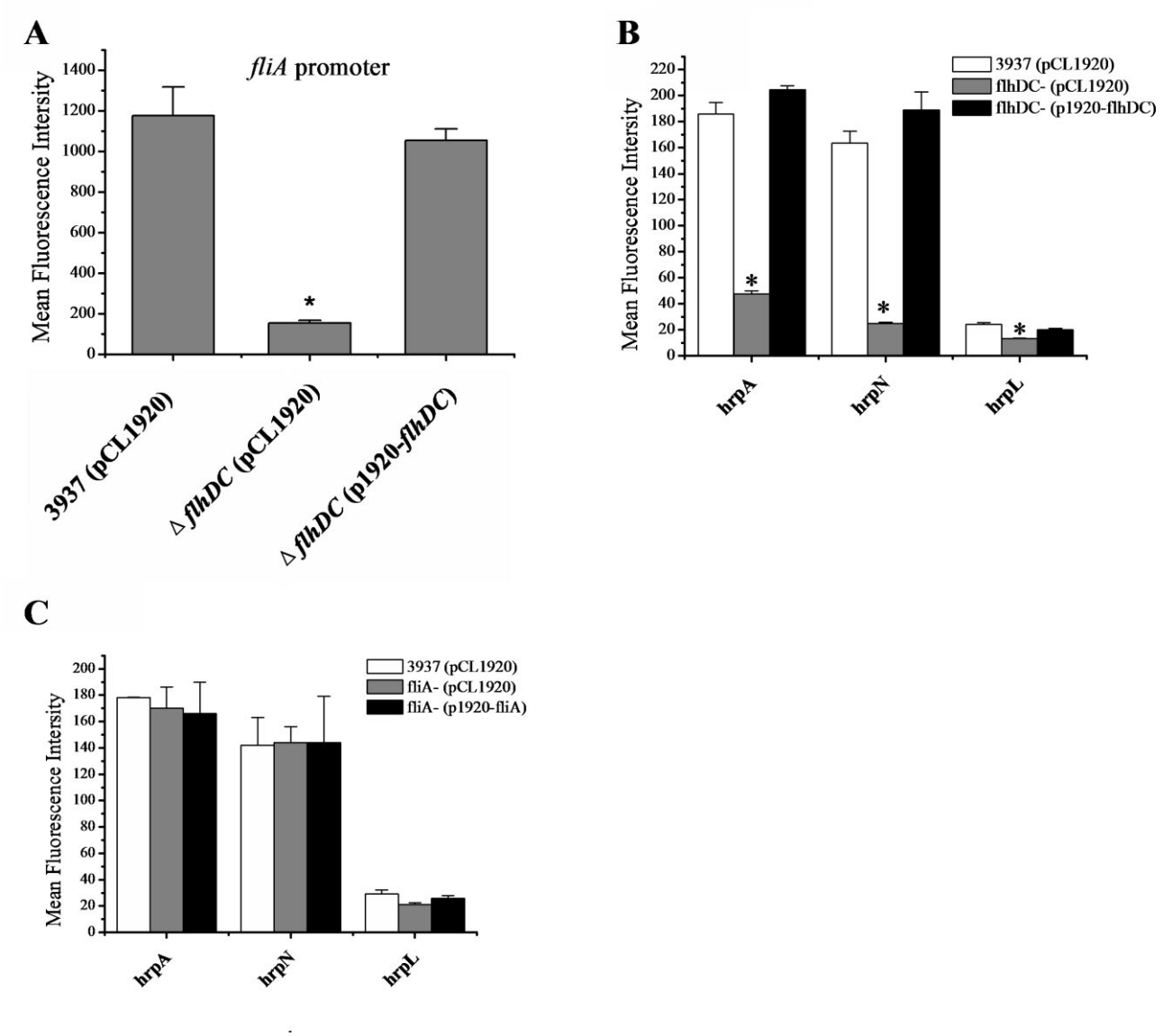

Fig. 5. The impact of mutation of *flhDC* and *fliA* on the T3SS gene expression in *D. dadantii* 3937 was examined.
A. Promoter activity of *fliA* was measured using plasmid pAT-*fliA* in wild-type strain *D. dadantii* harbouring empty vector pCL1920, the Δ*flhDC* harbouring empty vector pCL1920 and Δ*flhDC* harbouring pCL-*flhDC*.
B and C. Promoter activity of T3SS regulon genes *hrpA*, *hrpN* and *hrpL* was measured in the *D. dadantii* 3937 harbouring empty vector pCL1920, the Δ*flhDC* harbouring empty vector pCL1920, the Δ*fliA* harbouring empty vector pCL1920, and their complemented strains using reporter plasmids pAT-*hrpA*, pAT-*hrpN* and pAT-*hrpL* respectively. Three independent experiments were performed and three replicates were used in each experiment. Values are a representative of three experiments. Error bars indicate standard errors of the means. Asterisks indicate statistically significant differences of the means ($P < 0.05$ by Student's *t*-test).

conditions (Fig. 5B). Complementation of Δ*flhDC* by expression of *flhDC in trans* restored the *hrpL*, *hrpA* and *hrpN* promoter activities to the wild-type level (Fig. 5B). In contrast, similar promoter activities for *hrpL*, *hrpA* and *hrpN* were observed between the wild-type and Δ*fliA* strains (Fig. 5C), suggesting that FliA does not impact on T3SS gene expression. These results implied that FlhDC positively controlled the expression of T3SS independently of FliA.

FlhDC controls expression of ecpC*,* $ycgR_{3937}$*, but not* egcpB

The data above illustrated that the c-di-GMP degrading enzymes EGcpB and EcpC positively regulated the expression of T3SS, while $YcgR_{3937}$ partially mediated the regulatory pathway downstream of EGcpB. In addition, the flagellar master regulator FlhDC also positively regulated T3SS gene expression. To understand the

regulatory connections between these systems, we further examined the expression status of *ecpC*, *egcpB* and *ycgR*$_{3937}$ in the Δ*flhDC* and Δ*fliA* mutants. As shown in Fig. 6A, the promoter activity of *ecpC* dropped by 70% in the Δ*flhDC* mutant, but was not significantly affected in Δ*fliA*, suggesting that FlhDC positively regulated the expression of *ecpC*, and the regulation was probably independent of FliA. In comparison, the promoter activity of *egcpB* was not affected by mutation of either *flhDC*, or *fliA* (Fig. 6B), while that of *ycgR*$_{3937}$ was reduced in both Δ*flhDC* and Δ*fliA* (Fig. 6C). These results indicated that expression of *egcpB* was not regulated by FlhDC or FliA, and FlhDC positively regulated the expression of *ycgR*$_{3937}$ through FliA.

FlhDC positively controls the expression of the PDE *ecpC* (Fig. 6A) and the T3SS gene *hrpL* (Fig. 5B). As EcpC positively regulates an alternative sigma factor RpoN, which is required to activate the transcription of *hrpL* in *D. dadantii* 3937 (Yi *et al*., 2010), we hypothesized that FlhDC exerted its effects on T3SS gene expression via induction of *ecpC*. To test whether FlhDC regulates T3SS gene expression by activating the expression of *hrpL* through EcpC, a quantitative real time reverse transcription polymerase chain reaction (RT-PCR) was performed to measure the levels of *rpoN* and *hrpL* transcripts in the wild type and Δ*flhDC* mutant. As shown in Fig. 6D, a considerable decrease in the *rpoN* and *hrpL* transcript level was detected in Δ*flhDC* compared with the wild-type strain. Taken together, these results strongly suggest that FlhDC regulates T3SS gene expression through the FlhDC-EcpC-RpoN-HrpL pathway independently of FliA.

FlhDC positively controls rsmB *expression at the post-transcriptional level*

The GacS/A-*rsmB*-RsmA network has been well studied as a major regulatory pathway controlling the T3SS of *D. dadantii* (Yang *et al*., 2008b). In *P. carotovorum*, FlhDC promotes the transcription of *gacA* via an unknown mechanism, which in turn positively controls the expression of *rsmB* (Cui *et al*., 2008). Therefore, to investigate whether and at which level FlhDC regulates RsmB, we first examined the promoter activity of *rsmB* in the wild-type, Δ*flhDC* and Δ*fliA* strains under T3SS-inducing conditions. Interestingly, no difference in *rsmB* promoter activity was detected between the wild type and the mutants (Fig. 7A). We then monitored the RNA levels of *rsmB* in the above-mentioned strains by Northern blotting. The results showed that *rsmB* RNA level was reduced in Δ*flhDC*, but increased in Δ*fliA* when compared with the wild type (Fig. 7B). Complementation assays using low copy number plasmid pCL1920 containing *flhDC* and *fliA* genes restored the Δ*flhDC* and Δ*fliA* phenotypes to the wild-type levels respectively (Fig. 7B). RsmB positively regulates the production of pectate lyase by sequestering the effect of the post-transcriptional regulator RsmA (Yang *et al*., 2008b). To further investigate the impact of FlhDC and FliA on RsmB, we used a spectrophotomeric assay to monitor the pectate lyase production of wild-type, Δ*flhDC* and Δ*fliA* strains and the complemented strains. The results showed that the pectate lyase production was reduced in Δ*flhDC* while increased in Δ*fliA* compared with the wild-type strain (Fig. 7C). To conclude, we propose that FlhDC and FliA divergently post-transcriptionally regulate the *rsmB* RNA level in *D. dadantii* 3937, and that these effects may contribute to the attenuated T3SS gene expression in Δ*flhDC*.

FlhDC regulates T3SS gene expression mainly through EcpC

The findings outlined above revealed three potential pathways through which FlhDC regulated T3SS gene expression. They are the FlhDC-FliA-YcgR$_{3937}$ pathway, the FlhDC-EcpC-RpoN-HrpL pathway and the FlhDC-*rsmB*-RsmA-HrpL pathway respectively. To determine which pathway is the most dominant one, we first excluded the FlhDC-FliA-YcgR$_{3937}$ pathway. This is because a negative impact on the T3SS through YcgR$_{3937}$ was observed (Fig. 4B), which is in contrast to the phenotype in Δ*flhDC* in which the T3SS gene expression levels were lower than the wild type (Fig. 5B). Next, to compare the other two pathways, FlhDC-EcpC-RpoN-HrpL and FlhDC-*rsmB*-RsmA-HrpL, we engineered two constructs containing genes *ecpC* and *rsmB in trans* using low copy number plasmid pCL1920 respectively. The resulting plasmids were transferred into wild-type and Δ*flhDC* strains harbouring a *hrpA-gfp* reporter plasmid pAT-*hrpA*. The results for transcriptional assays showed that Δ*flhDC* strain with plasmid pCL1920 expressing *rsmB* was unable to restore the *hrpA* promoter activity to the wild-type level. In contrast, Δ*flhDC* strain with the plasmid pCL1920 expressing *ecpC* restored the *hrpA* promoter activity to the wild-type level (Fig. 8). Based on these results, we concluded that the positive effect of *D. dadantii* 3937 FlhDC on T3SS gene expression was mainly controlled through the FlhDC-EcpC-RpoN-HrpL pathway.

Motility regulators are required for the virulence of D. dadantii

Since FlhDC and FliA affected multiple phenotypes, such as swimming motility (Fig. S2), pectate lyase production and T3SS, which have been known to contribute to *D. dadantii* pathogenesis (Beaulieu and Van Gijsegem, 1990; Yang *et al*., 2002; Antúnez-Lamas *et al*., 2009), virulence assays were performed to assess the effects of Δ*flhDC* and Δ*fliA* in the leaves of host plant Chinese

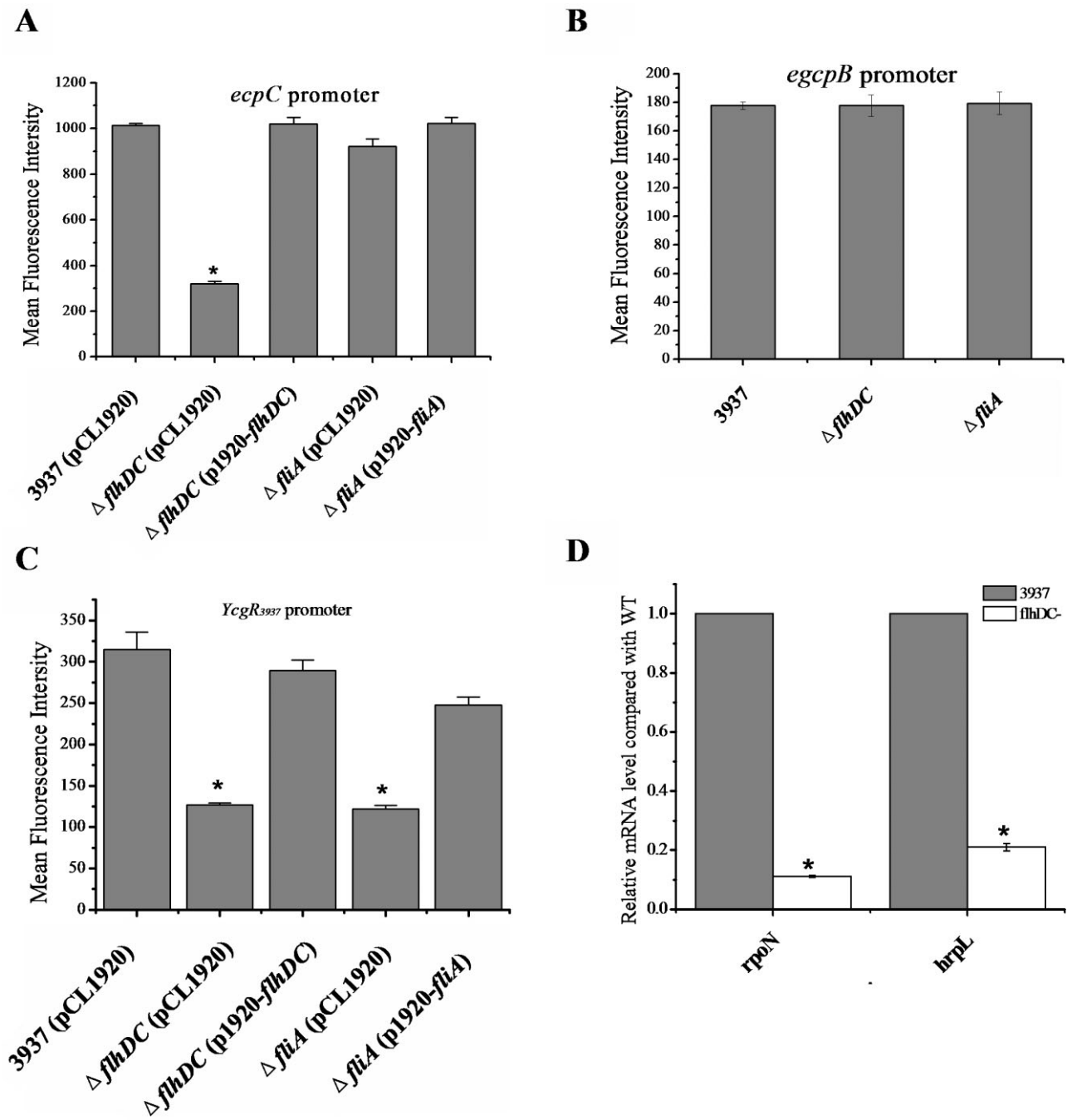

Fig. 6. FlhDC, independently of FliA, regulates the T3SS master regulator HrpL at transcriptional level through EcpC-RpoN-HrpL pathway in *D. dadantii* 3937. But FlhDC positively regulates transcription of $ycgR_{3937}$ through FliA.
A. Promoter activity of *ecpC* was measured in the wild-type *D. dadantii*, the *flhDC* and *fliA* mutant strains and the *flhDC* and *fliA* complemented strains respectively.
B. Promoter activity of *egcpB* was measured in wild-type *D. dadantii*, Δ*flhDC* and Δ*fliA* strains.
C. Promoter activity of $ycgR_{3937}$ was measured in wild-type *D. dadantii* harbouring empty vector pCL1920, the Δ*flhDC* harbouring empty vector pCL1920, the Δ*fliA* harbouring empty vector pCL1920 and their complemented strains.
D. Relative mRNA levels of *hrpL* and *rpoN* were examined using quantitative real time RT-PCR in the wild-type *D. dadantii* and the Δ*flhDC*.
Values are a representative of three independent experiments. Three replicates were used in each experiment. Error bars indicate standard errors of the means. Asterisks indicate statistically significant differences of the means ($P < 0.05$ by Student's *t*-test).

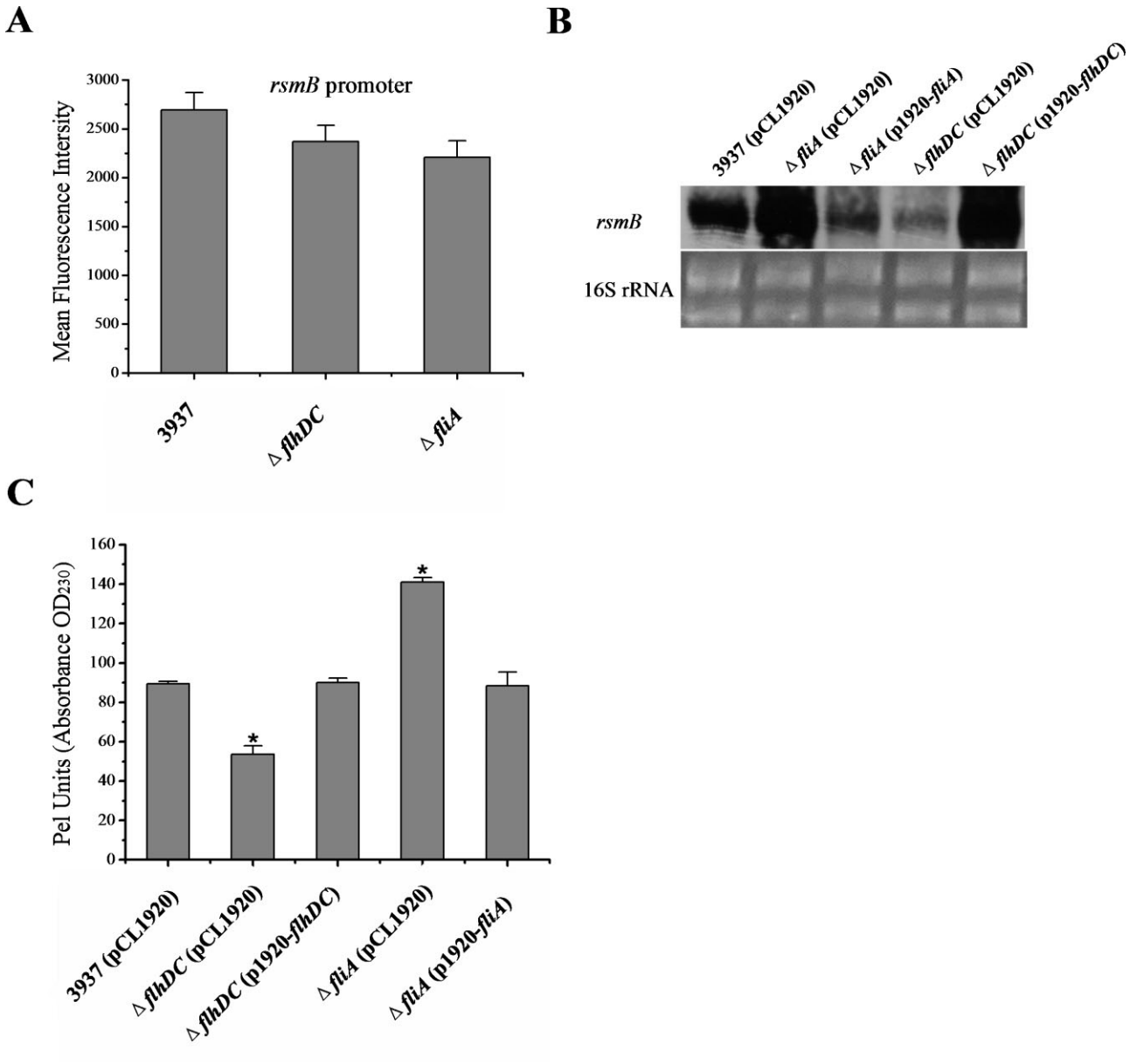

Fig. 7. FlhDC and FliA inversely regulate RsmB at a post-transcriptional level.
A. Promoter activity of *rsmB* was measured in the wild-type *D. dadantii*, the *flhDC* mutant and the *fliA* mutant strains.
B. Northern blot analysis of *rsmB* mRNA in the wild-type *D. dadantii* harbouring empty vector pCL1920, Δ*fliA* harbouring empty vector pCL1920, Δ*fliA* harbouring plasmid pCL1920-*fliA*, Δ*flhDC* harbouring empty pCL1920 and Δ*flhDC* harbouring pCL1920-*flhDC*. 16S rRNA was used as RNA loading control.
C. Pectate lyase production assay was performed in the wild-type *D. dadantii* harbouring empty vector pCL1920, Δ*fliA* harbouring empty vector pCL1920, Δ*fliA* harbouring plasmid pCL1920-*fliA*, Δ*flhDC* harbouring empty pCL1920 and Δ*flhDC* harbouring pCL1920-*flhDC*. Values are a representative of three independent experiments. Three replicates were used in each experiment. Error bars indicate standard errors of the means. Asterisks indicate statistically significant differences of the means ($P < 0.05$ by Student's *t*-test).

cabbage (*Brassica campestris*). Compared with the wild type, deletion mutants of *flhDC* and *fliA* were significantly reduced in maceration ability in planta (Fig. 9). Complementation assays restored the mutant phenotypes to the wild-type level. Similar results were also observed in African violet (*Saintpaulia ionantha*) when inoculated with these bacterial strains (Fig. S3). These data suggested that FlhDC and FliA are both essential for the full pathogenesis of *D. dadantii* 3937.

Since the findings outlined above showed that FlhDC and FliA regulated swimming motility in the same direction, but not pectate lyase production or T3SS, we speculated that motility might play a determinate role in the FlhDC-regulated virulence. When *ecpC* was expressed *in*

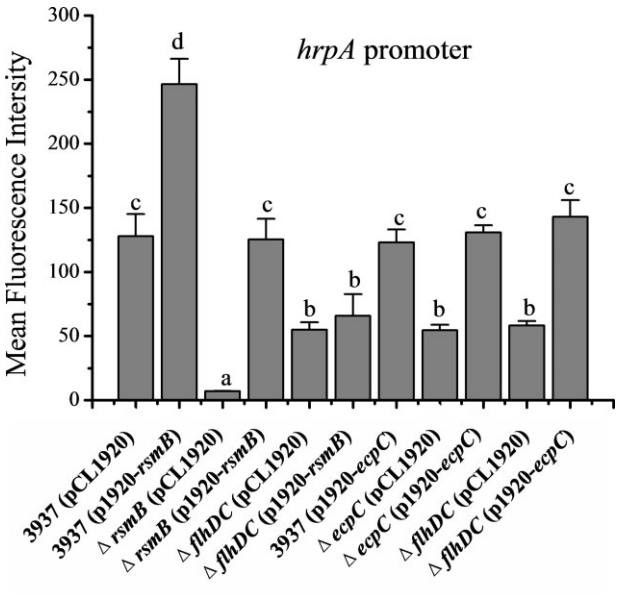

Fig. 8. Promoter activity of *hrpA* in different *D. dadantii* 3937 strains was examined. Values are a representative of three independent experiments. Three replicates were used in each experiment. Error bars indicate standard errors of the means. Different lowercase letters above the bar indicate statistically significant differences between treatments ($P < 0.05$ by Student's *t*-test).

trans in Δ*flhDC*, it restored *hrpA* promoter activity and pectate lyase production (Fig. 8 and Fig. S4A). In contrast, expression of *rsmB* in Δ*flhDC* was able to restore pectate lyase production, but not T3SS gene expression (Fig. 8 and Fig. S4A). However, neither *ecpC* nor *rsmB* expression restored the swimming motility in Δ*flhDC* (Fig. S4B), which suggests that FlhDC, the flagellar master regulator, controls flagellar gene expression independent of EcpC or RsmB. As expected, neither *ecpC* nor *rsmB* expression in Δ*flhDC* strain restored its virulence in the leaves of Chinese cabbage (Fig. 9). These results supported the statement that motility is essential for the FlhDC-regulated virulence.

Discussion

In this study, we identified two PilZ-domain proteins $YcgR_{3937}$ and $BcsA_{3937}$ in *D. dadantii* 3937 and demonstrated that these proteins regulated diverse cellular activity under elevated c-di-GMP conditions. $YcgR_{3937}$ specifically bound c-di-GMP as an effector both *in vivo* and *in vitro*, and this binding ability was required for mediating the regulation of T3SS gene expression by EGcpB. In addition, we demonstrated that the flagellar master regulator FlhDC regulated T3SS gene expression mainly through induction of the PDE *ecpC* under our experimental conditions.

We detected increased c-di-GMP concentrations in the PDE mutants including Δ*egcpB*, Δ*ecpC* and Δ*egcpB*Δ*ecpC* (Fig. 1), which confirmed that EGcpB and EcpC regulated various cellular activities by modulating c-di-GMP levels. It has been proposed in many bacterial species that the regulation of c-di-GMP signalling is controlled in a temporal and spatial manner in the cell (Hengge, 2009). EGcpB and EcpC probably control the degradation of c-di-GMP derived from different c-di-GMP pools, since deleting two of them had an additive effect on the increase of overall cellular c-di-GMP level. The changes in the c-di-GMP level are sensed at least partially by two PilZ domains proteins $YcgR_{3937}$ and $BcsA_{3937}$, since further deletion of them in the individual PDE mutants could restore some of the phenotypes to near wild-type level (Fig. 3B–F).

In *E. coli* and *Salmonella*, the regulatory role of YcgR was found to be strictly associated with motility (Ryjenkov *et al.*, 2006; Fang and Gomelsky, 2010; Paul *et al.*, 2010). Here, we showed $YcgR_{3937}$ not only regulated bacterial motility, but was mainly involved in the regulation of other activities including biofilm formation, pectate lyase production and T3SS gene expression (Figs 3 and 4). This is

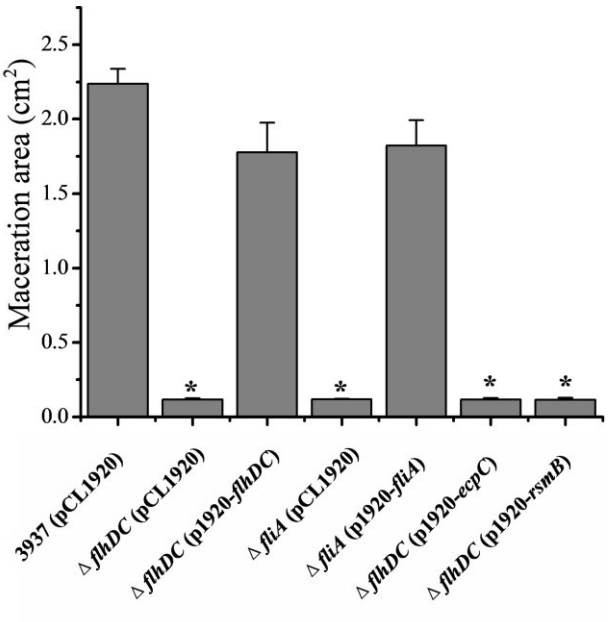

Fig. 9. FlhDC and FliA positively regulate the virulence of *D. dadantii* 3937 on Chinese cabbage (*Brassica campestris*). Bacterial cells of the wild-type *D. dadantii* harbouring empty vector pCL1920, Δ*fliA* harbouring empty vector pCL1920, Δ*fliA* harbouring plasmid pCL1920-*fliA*, Δ*flhDC* harbouring empty pCL1920, Δ*flhDC* harbouring pCL1920-*flhDC*, Δ*flhDC* harbouring pCL1920-*ecpC* and Δ*flhDC* harbouring pCL1920-*rsmB* strains were inoculated in the leaves of Chinese cabbage. The maceration symptom was measured 24 h post-inoculation. Maceration assays were performed as described in the *Experimental procedures*. Error bars indicate standard errors of the means. Asterisks indicate statistically significant differences of the means ($P < 0.05$ by Student's *t*-test).

probably due to differences in the c-di-GMP signalling network between different bacterial species. In addition, $YcgR_{3937}$ positively regulated T3SS gene expression in the Δ*egcpB* background, but not the Δ*ecpC* background, suggesting that EGcpB and EcpC might have different mechanism in affecting T3SS gene expression. Whether there are other c-di-GMP effectors mediating the downstream signalling pathway of EcpC needs further investigation.

BcsA in *E. coli* and *Salmonella* strains was shown to play a role in synthesizing cellulose, a major component of the extracellular matrix (Zogaj *et al*., 2001; Hengge, 2009; Zorraquino *et al*., 2013). Here, we showed $BcsA_{3937}$ regulated biofilm formation and pectate lyase production under the elevated levels of c-di-GMP (Fig. 3B and C), which is similar to $YcgR_{3937}$. $BcsA_{3937}$ of *D. dadantii* positively regulates biofilm formation which might be due to the ability of $BcsA_{3937}$ to produce cellulose when c-di-GMP is elevated (Jahn *et al*., 2011). Dissimilar to $YcgR_{3937}$, $BcsA_{3937}$ was not shown to affect the regulation of motility (Fig. 3A). A recent study in *Salmonella* demonstrated that BcsA and YcgR coordinately regulate swimming motility, in which BcsA produces cellulose to block the rotation of flagellar (Zorraquino *et al*., 2013). It is possible that, similar to *Salmonella*, $BcsA_{3937}$ regulates swimming motility in Δ*ycgR* background under high-c-di-GMP-level condition. Moreover, $BcsA_{3937}$ and $YcgR_{3937}$ regulated T3SS gene expression in opposite directions in the Δ*egcpB* and Δ*ecpC* backgrounds (Fig. 4). These data suggest that the regulation of T3SS by c-di-GMP signalling system in *D. dadantii* involves multiple components and is very complex.

It has been shown that YcgR interacted with the flagellar switch complex proteins FliG and FliM to regulate swimming motility (Fang and Gomelsky, 2010; Paul *et al*., 2010). The point mutation R118D in the RxxxR motif of YcgR abolished it binding ability to c-di-GMP, and also weakened its binding to FliM or FliG, suggesting that the c-di-GMP binding ability of YcgR is required for its strong interaction with flagellar switch complex in responding to intracellular c-di-GMP changes (Fang and Gomelsky, 2010; Paul *et al*., 2010). Here, our *in vitro* ITC and *in vivo* FRET assays confirmed that $YcgR_{3937}$ is a c-di-GMP binding protein, and the RxxxR motif in the PilZ domain is required for the binding activity (Table 1 and Fig. S1). In addition, by chromosomally replacing the wild-type $YcgR_{3937}$ with $YcgR_{3937}^{R124D}$, we showed that the binding to c-di-GMP is essential for its regulatory role on T3SS gene expression (Fig. 4B). Recently, Morgan and colleagues presented crystal structures of the c-di-GMP-activated BcsA complex, which confirmed that the biological activity of BcsA is promoted through the allosteric effect of c-di-GMP (Morgan *et al*., 2014). We tried to examine whether the binding ability of PilZ domain of $BcsA_{3937}$ to c-di-GMP is responsible for the phenotypes of biofilm formation, pectate lyase production and T3SS expression. However, several attempts of integrating the $bcsA_{3937}$ gene with amino acid replacements in the PilZ motif into the chromosome of the *D. dadantii* were unsuccessful. In addition, the ITC and FRET assays were not performed in $BscA_{3937}$ as a result that overexpression of $BcsA_{3937}$ in the *E. coli* cloning strain led to the poor growth and dead of the bacteria.

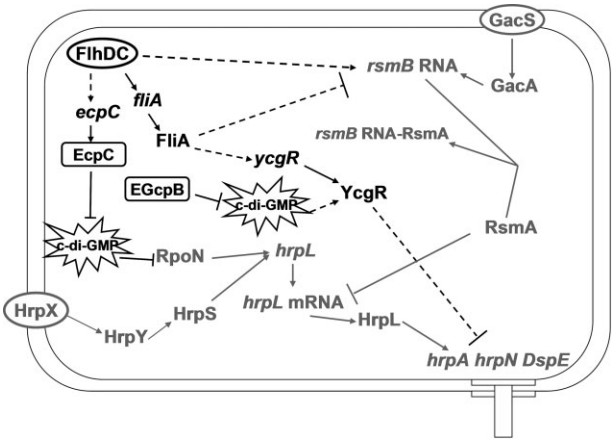

Fig. 10. Model for the type III secretion system (T3SS) regulatory network in *D. dadantii* 3937. The *D. dadantii* 3937 T3SS is regulated by the HrpX/HrpY-HrpS-HrpL and the GacS/GacA-*rsmB*-RsmA-HrpL pathways. In this study, the flagellar master regulator FlhDC was observed to hierarchically regulate the expression of T3SS encoding genes. (i) FlhDC positively regulates the PilZ domain protein encoding gene $ycgR_{3937}$ at transcriptional level through a sigma factor FliA. Under high c-di-GMP levels (Δ*egcpB*), $YcgR_{3937}$ binds c-di-GMP, which negatively regulates the T3SS. (ii) FlhDC controls the expression of phosphodiesterase encoding gene *ecpC*. EcpC degrades intracellular c-di-GMP, which counteracts the negative impact of c-di-GMP on the RpoN, which is required for the transcription of *hrpL*. (iii) FlhDC and FliA divergently regulate the regulatory small RNA RsmB at the post-transcriptional level. ⊥represents negative control; → represents positive control. The dotted lines indicate regulatory mechanisms identified in this study.

We demonstrated that the flagellar master regulator FlhDC played a role in regulating T3SS gene expression. Three unique pathways were uncovered, including the FlhDC-FliA-$YcgR_{3937}$ pathway, the FlhDC-EcpC-RpoN-HrpL pathway and the FlhDC-*rsmB*-RsmA-HrpL pathway and a model of FlhDC regulation of T3SS genes was developed (Fig. 10). In the first regulatory pathway, the FlhDC controlled sigma-factor FliA activates the expression of $ycgR_{3937}$ at the transcriptional level. Under Δ*egcpB*-mediated high-c-di-GMP-level condition, $YcgR_{3937}$ binds c-di-GMP and negatively regulates the expression of T3SS regulon gene *hrpA*. Although the regulatory effect of YcgR on T3SS was not reported previously, the FlhDC-FliA-YcgR pathway was identified in *S.* Typhimurium (Frye *et al*., 2006). In the FlhDC-EcpC-RpoN-HrpL pathway, FlhDC controls the expression of *ecpC*, a phosphodiesterase encoding gene at transcriptional level. EcpC lowers the intracellular c-di-GMP

concentration by degrading c-di-GMP, which positively affects the transcription of *hrpL* through the sigma factor RpoN at post-transcriptional level (Fig. 6A and D) (Yi *et al*., 2010). It is important to note that this regulation is different in *E. coli*, where the expression of *yhjH* (*ecpC* homologue) of *E. coli* is activated by FliA (Pesavento *et al*., 2008), as the expression of *ecpC* of *D. dadantii* is regulated by FlhDC but independent of FliA (Fig. 6A). In addition, computational and DNase footprinting analyses in *E. coli* and *S.* Typhimurium of the FlhDC-regulon gene promoter regions have identified a consensus FlhDC binding sequence, in which two repeats of FlhDC-binding boxes AA(C/T)G(C/G)$N_{2\text{-}3}$AAATA(A/G)CG are separated by a non-conserved 10–12 nucleotides (Claret and Hughes, 2002; Stafford *et al*., 2005). In our work, we did not find this binding sequence within the 500bp from the 5′ *ecpC* start codon, suggesting that FlhDC might not directly activate *ecpC* by binding to its promoter region. Finally, in the FlhDC-*rsmB*-RsmA-HrpL pathway, we discovered that FlhDC positively regulates the production of RsmB RNA at post-transcriptional level, while FliA negatively regulates it (Fig. 7B). RsmB binds to RsmA, which neutralizes RsmA's negative impact on *hrpL* mRNA (Liu *et al*., 1998; Chatterjee *et al*., 2002). In *P. carotovorum*, FlhDC was reported to positively regulate *rsmB* through the *rsmB* transcriptional activator GacA at transcriptional level (Cui *et al*., 2008). The promoter activity of *rsmB* is controlled by GacA in *D. dadantii* (Yang *et al*., 2008b). However, we did not detect any significant impact on the promoter activity of *rsmB* from the deletion of either *flhDC* or *fliA* (Fig. 7A), suggesting that despite the overall impact of FlhDC on *rsmB* are same between *P. carotovorum* and *D. dadantii*, the regulatory mechanisms behind are different. Furthermore, since RsmB has also been reported to positively regulate the production of pectate lyase in *D. dadantii* (Yang *et al*., 2008b), our observation that the pectate lyase production increased in Δ*fliA* compared with the wild-type strain is in agreement with the earlier statement. Owing to the fact that FlhDC also regulates the expression of the phosphodiesterase encoding gene *ecpC* (Fig. 6A), the reduced pectate lyase production observed in Δ*flhDC* may be due to a coordinated regulation of FlhDC on both the *rsmB*-RsmA system and the c-di-GMP signalling system (Yi *et al*., 2010). Expressing *ecpC* or *rsmB* using plasmid pCL1920 in Δ*flhDC* strain restored the pectate lyase production to near wild-type level, respectively (Fig. S4A), which has proved the above hypothesis. Finally, since we observed that FlhDC hierarchically regulates the expression of T3SS encoding genes, we further determined which of the three components, $YcgR_{3937}$, EcpC or *rsmB*, contributes to the FlhDC's positive effect on the T3SS. We first excluded $YcgR_{3937}$ due to its negative impact on the T3SS. Our results showed that expression of *ecpC* using low copy number plasmid pCL1920 under the Δ*flhDC* background is able to restore the promoter activity of T3SS encoding gene *hrpA* to the wild-type level (Fig. 8). No significant difference was detected when *rsmB* was expressed under the same condition (Fig. 8). To conclude, these data suggest that the regulation of FlhDC on T3SS is mainly through the FlhDC-EcpC-RpoN-HrpL pathway.

Previous studies in *D. dadantii* 3937 demonstrated that swimming motility, pectate lyase production and the T3SS are essential virulence factors that contribute to the pathogenicity of *D. dadantii* in host plant (Bauer *et al*., 1994; Yang *et al*., 2002; 2008b; Antúnez-Lamas *et al*., 2009). Here, we uncovered a master regulator FlhDC, which positively regulates swimming motility, pectate lyase production and T3SS expression (Fig. S2, 5B and 7C). The sigma-factor FliA was found to positively regulate swimming motility but negatively regulates pectate lyase production and has no impact on T3SS expression (Fig. S2, 5C and 7C). Interestingly, our results showed significant reductions in maceration ability in planta for both Δ*flhDC* and Δ*fliA* strains (Fig. 9 and Fig. S3). We also observed that expression of *ecpC in trans* in Δ*flhDC* restored *hrpA* promoter activity and pectate lyase production (Fig. 8 and Fig. S4A), but not swimming motility or overall virulence in Chinese cabbage (Fig. 9 and Fig. S4B). In addition, expression of *rsmB in trans* in Δ*flhDC* restored only pectate lyase production, but not *hrpA* promoter activity, swimming motility or virulence in Chinese cabbage (Figs 8 and 9, Fig. S4A and B). Thus, these results together with the previous report that several motility-deficient mutants were severely impaired in virulence (Antúnez-Lamas *et al*., 2009), implied that the reduced virulence of Δ*flhDC* and Δ*fliA* strains might be due to their defectiveness in swimming motility, which is why they cannot be restored by pectate lyase production or T3SS gene expression. Therefore, we conclude that the swimming motility, pectate lyase production and T3SS gene expression are essential in determining the full virulence of *D. dadantii* 3937 in host plants.

Many studies have demonstrated that the bacterial T3SS and the flagellum are evolutionarily related, since they share similarities in structure, function and sequences of the main components (Young *et al*., 1999; Lee and Galán, 2004; Pallen *et al*., 2005; Erhardt *et al*., 2010). In *Salmonella*, the type III effector SptP missing its chaperone-binding domain was secreted through the flagellar system instead of the T3SS, implying that these effectors carry ancient signals that could be recognized by the flagellar system (Lee and Galán, 2004). Recently, it was demonstrated that the flagellin protein FliC in *Pseudomonas syringae* could be translocated into plant cells by the T3SS and induce immune responses (Wei *et al*., 2013). Here, our work provides novel insights that further support a connection between flagella and T3SS

by showing that the flagellar master regulator FlhDC of *D. dadantii* 3937 also regulates the transcription of the T3SS in a c-di-GMP-dependent manner.

Experimental procedures

Bacterial strains, plasmids, primers and media

The bacterial strains and plasmids used in this study are listed in Table S1 (see Supporting Information). *Dickeya dadantii* 3937 and mutant strains were stored at −80°C in 20% glycerol. *Dickeya dadantii* strains were grown in Luria–Bertani (LB) medium (1% tryptone, 0.5% yeast extract and 1% NaCl), mannitol-glutamic acid (MG) medium (1% mannitol, 0.2% glutamic acid, 0.05% potassium phosphate monobasic, 0.02% NaCl and 0.02% $MgSO_4$) or low nutrient T3SS inducing minimal medium (MM) at 28°C (Yang *et al*., 2007; 2008b). *Escherichia coli* strains were grown in LB at 37°C. Antibiotics were added to the media at the following concentrations: ampicillin (100 μg ml^{-1}), kanamycin (50 μg ml^{-1}), gentamicin (10 μg ml^{-1}), chloramphenicol (20 μg ml^{-1}), tetracycline (12 μg ml^{-1}) and spectinomycin (100 μg ml^{-1}). The *D. dadantii* 3937 genome sequence can be retrieved from a systematic annotation package for community analysis of genomes (ASAP) (https://asap.ahabs.wisc.edu/asap/home.php). Primers used for PCR in this report are listed in Table S2 (see Supporting Information).

Mutant construction and complementation

The *flhDC*, *fliA*, $bcsA_{3937}$ and $ycgR_{3937}$ genes were deleted from the genome by marker exchange mutagenesis (Yang *et al*., 2002). Briefly, two fragments flanking each target gene were amplified by PCR with specific primers (Table S2). The kanamycin cassette was amplified from pKD4 (Datsenko and Wanner, 2000), and was cloned between two flanking regions using three-way cross-over PCR. The PCR construct was inserted into the suicide plasmid pWM91, and the resulting plasmid was transformed into *D. dadantii* 3937 by conjugation using *E. coli* strain S17-1 λ-pir. To select strains with chromosomal deletions, recombinants, grown on kanamycin medium, were plated on 5% sucrose plate. Cells that were resistant to sucrose due to SacB-mediated toxicity were then plated on ampicillin plate, and the ampicillin sensitive cells were confirmed by PCR using outside primers. Finally, the DNA fragment which contains two flanking regions and kanamycin cassette was sequencing confirmed. To generate complemented strains, the promoter and open reading frame region of target genes were amplified and cloned into low copy number plasmid pCL1920 (Table S1). The resulting plasmids were then confirmed by PCR and electroporated into mutant cells.

Biofilm formation assay

Biofilm formation was determined by using a method that was previously described (Yi *et al*., 2010). In brief, bacterial cells grown overnight in LB media were inoculated 1:100 in MM media in 1.5 ml polypropylene tubes. After incubation at 28°C for 48 h, cells were stained with 1% crystal violet (CV) for 15 min. The planktonic cells were removed by several rinses with H20. The CV-stained bound cells were air dried for 1 h, then dissolved in 90% ethanol, and the optical density 590 (OD590) of the solution was measured to quantify the biofilm formation.

Swimming motility assay

Swimming motility was tested by inoculating 10 μl of overnight bacterial cultures (OD_{600} = 1.0) onto the center of MG plates containing 0.2% agar. The inoculated plates were incubated at 28°C for 20 h, and the diameter of the radial growth was measured (Antúnez-Lamas *et al*., 2009).

Pectate lyase activity assay

Extracellular Pel activity was measured by spectrometry as previously described (Matsumoto *et al*., 2003). Briefly, bacterial cells were grown in MM media supplemented with 20% glycerol and 1% polygalacturonic acid at 28°C for 20 h. For extracellular pel activity, 1 ml bacterial cultures were centrifuged at 15000 r.p.m. for 2 min, supernatant was then collected, and 10 μl of the supernatant was added to 990 μl of the reaction buffer (0.05% PGA, 0.1 M Tris-HCl [pH 8.5] and 0.1 mM $CaCl_2$, pre-warmed to 30°C). Pel activity was monitored at A_{230} for 3 min and calculated based on one unit of Pel activity equals to an increase of 1×10^{-3} OD_{230} in 1 min.

Green fluorescent protein (GFP) reporter plasmid construction and flow cytometry assay

To generate the reporter plasmids pAT-$ycgR_{3937}$ and pAT-*ecpC*, the promoter regions of $ycgR_{3937}$ and *ecpC* were PCR amplified and cloned into the promoter probe vector pPROBE-AT, which contains the ribosomal binding site upstream of the *gfp* gene respectively (Miller *et al*., 2000; Leveau and Lindow, 2001). The reporter plasmids pAT-*hrpA*, pAT-*hrpN*, pAT-*hrpL* and pAT-*rsmB* were constructed previously following the same procedure (Yang *et al*., 2007; Li *et al*., 2014). Promoter activity was monitored by measuring GFP intensity through flow cytometry (BD Biosciences, San Jose, CA) as previously described (Peng *et al*., 2006). Briefly, bacterial cells with reporter plasmid were grown in LB media overnight and inoculated 1:100 into MM media. Samples were collected at 12 h and 24 h, respectively, and promoter activity was analysed by detecting GFP intensity using flow cytometry.

Determination of intracellular c-di-GMP concentration

Intracellular c-di-GMP concentrations were determined by using ultra performance liquid chromatography coupled with tandem mass spectrometry (UPLC-MS-MS), that has been described previously (Edmunds *et al*., 2013). Overnight bacterial cultures were inoculated 1:100 into 30 ml LB media in a flask. After checking OD_{600} of bacterial culture reached about 0.8, corresponding to mid- to late-exponential growth, all cells were centrifuged in 50 ml polystyrene centrifuge tubes for 30 min at 4000 r.p.m. The supernatant was then removed,

and the pellet was re-suspended in 1.5 ml extraction buffer (40% acetonitrile–40% methanol in 0.1 N formic acid). To lyse the cell and release intracellular c-di-GMP, cells re-suspended in extraction buffer were left at −20°C for 30 min, and then centrifuged at 13 000 r.p.m for 1 min. The supernatant was collected and analysed by UPLC-MS-MS.

Protein expression and purification

The full length of $ycgR_{3937}$ was cloned into the expression vector pET21b by primers $ycgR_{3937}$-for-NdeI and $ycgR_{3937}$-rev-EcoRI (Table S2). To construct the point-specific mutation in the RxxxR motif of $YcgR_{3937}$ PilZ domain, single nucleotide substitution was performed using the QuikChange XL Site-Directed Mutagenesis Kit (Agilent, Santa Clara, CA). Briefly, a primer set, $ycgR_{3937}$-R124D-1 and $ycgR_{3937}$-R124D-2 (Table S2), was used to generate $ycgR_{3937}^{R124D}$, which changed the RxxxR motif to RxxxD. Substitution was confirmed by DNA sequencing. The constructs carrying $ycgR_{3937}$ and $ycgR_{3937}^{R124D}$ were transformed into *E. coli* BL21 stains for protein expression and purification. Briefly, expression of fusion proteins was induced by addition of isopropyl-thio-galactopyranoside at a final concentration of 0.5 mM, and the bacterial cultures were then incubated at 16°C for 12 h. Then bacterial cells were collected by centrifugation, followed by suspension in phosphate buffered saline and sonication. The crude cell extracts were centrifuged at 12 000 r.p.m. for 25 min to remove cell debris. The supernatant containing the soluble proteins was collected and mixed with pre-equilibrated Ni^{2+} resin (GE Healthcare, Piscataway, NJ, USA) for 3 h at 4°C, then placed into a column and extensively washed with buffer containing 30 mM Tris-HCl (pH 8.0), 350 mM NaCl, 0.5 mM EDTA, 10% glycerol, 5 mM $MgCl_2$ and 30 mM imidazole. The proteins were subsequently eluted with buffer containing 300 mM imidazole. The purified proteins were analysed by sodium dodecyl sulfate polyacrylamide gel electrophoresis.

ITC assay

The binding of $YcgR_{3937}$ and $YcgR_{3937}^{R124D}$ to c-di-GMP was detected on ITC200 (MicroCal, Northampton, MA) following the manufacturer's protocol. In brief, 2 μl of c-di-GMP solution (500 μM) was injected at 2 min intervals via a 60 μl syringe into the sample cell containing $YcgR_{3937}$ or $YcgR_{3937}^{R124D}$ proteins (50 μM) with constant stirring at 20°C, and the heat change accompanying these additions were recorded. The titration experiment was repeated three times, and the data were calibrated with a buffer control and fitted with the single-site model to determine the binding constant (K_d) using the MicroCal origin version 7.0 software.

FRET analysis

To construct the c-di-GMP sensor *in vivo*, the plasmid pMMB67EHGent-$ycgR_{3937}$ (YFP-$YcgR_{3937}$-CFP), $ycgR_{3937}$ fragment was amplified using specific primers (Table S2) and cloned into pMMB67EHGent vector. The resulting plasmid was transferred into *D. dadantii* 3937 by electroporation. Bacterial strain containing the pMMB67EHGent vector or derivative plasmids was incubated in LB medium at 28°C with a range from 0 to 100 μM IPTG (Isopropyl β-D-1-thiogalactopyranoside) and 10 μg ml^{-1} gentamycin for both 12 h and 24 h to express various amounts of $YcgR_{3937}$-based c-di-GMP sensors. After incubation, the cells placed on a glass-bottom dish were ready for FRET imaging. Accurate determination of apparent FRET efficiency for cells expressing the $YcgR_{3937}$-based c-di-GMP sensor was performed by spectrally resolved FRET imaging (Raicu *et al*., 2009) using an optical micro-spectroscope (OptiMiS TruLine, Aurora Spectral Technologies, Milwaukee, WI). The imaging system was equipped with a Ti-Sapphire laser (Tsunami, Spectra-Physics) with a tuning range of 690–1040 nm and delivering pulses with a width of < 100 fs at a repetition rate of 80 MHz. In this system, the excitation beam is shaped into a line by employing a curved mirror placed at the back focal plane of the scanning lens (Biener *et al*., 2013). This set-up features a reduced acquisition time and increased overall sensitivity. The incident light is focused through an infinity-corrected oil-immersion objective (100 × magnification, NA 1.4, Nikon Instruments, Melville, NY) to a line with diffraction-limited thickness on the sample. The emitted light is passed through a transmission grating and projected onto a cooled electron-multiplying change-coupled device camera (EMCCD; Andor, iXon 897).

Dishes containing cells expressing the c-di-GMP sensor were placed on the microscope sample stage and irradiated at 800 nm with femtosecond light pulses to obtain emission spectra consisting of signals from donors and acceptors for every pixel in an image. Emission spectra also were separately acquired for cells expressing donors or acceptors alone, which were excited at 800 nm and 960 nm respectively; the measured fluorescence intensities were normalized to the maximum value to obtain elementary spectra for donors and acceptors. The elementary spectra where then used to unmix the donor and acceptor signals for the cells expressing the c-di-GMP sensor following a procedure described elsewhere (Raicu and Singh, 2013). The signals corresponding to the donor in the presence of acceptor (k^{DA}) and acceptor in the presence of donor (k^{AD}), respectively, were used to compute the FRET efficiency at each pixel in an image, using the same method as described before (Raicu *et al*., 2009).

For data analysis, an automatic computer algorithm, based on thresholding, masking and segmentation, was performed. First, an image was generated (labeled as F^D) by correcting for FRET the digital image of the donor in the presence of acceptor, k^{DA}, and multiplying by the donor spectral integral, as described elsewhere (Patowary *et al*., 2013). Then, a threshold for the donor emission, based on Otsu's algorithm, was chosen (Otsu, 1975). Next, a mask of the F^D image was formed using this threshold. The mask was segmented using a MATLAB function 'boundaries' (Gonzalez *et al*., 2004). The segments' boundaries were plotted to assist the user in removing segments containing multiple bacteria. Once the segments were approved by the user, the mask was used to select all the pixels corresponding to individual cells. Fluorescence images contained an average of 50 cells per image. Between 5 and 11 images were acquired for each sample type. Average FRET efficiency values were computed over all cells in an image and then mean values and standard errors of the mean (i.e. standard deviation divided by the square

root of the number of images) were computed for each sample type.

Northern blotting analysis

To measure the RNA levels of *rsmB* in wild type, Δ*flhDC*, Δ*fliA* and complemented strains, bacterial cells grown in MM for 12 h were harvested and total RNA was isolated using TRI reagent (Sigma-Aldrich, St Louis, MO). The residual DNA was removed with a Turbo DNA-free DNase kit (Ambion, Austin, TX). Northern blotting analysis was performed using biotin-labelled probe and a biotin detection system (BrightStar Psoralen-Biotin and Bright Star BioDetect, Ambion). 16S rRNA was used as an internal control.

qRT-PCR analysis

The mRNA levels of *rpoN* and *hrpL* were measured by qRT-PCR. Briefly, bacterial cells cultured in MM for 12 h were harvested and total RNA was isolated using RNeasy mini kit (Qiagen, Hilden, Germany) according to the manufacturer's instruction. Extracted RNA was treated with Turbo DNase I (Ambion, Austin, TX), and cDNA was synthesized using iScript cDNA synthesis kit (Bio-Rad Laboratories, Hercules, CA). The complementary (c)DNA level of target genes was quantified by qRT-PCR using a Real Master Mix (Eppendorf, Westbury, NY, USA), as described previously (Peng *et al*., 2006). Data were analysed using A RELATIVE EXPRESSION SOFTWARE TOOL (Pfaffl *et al*., 2002). The expression level of *rplU* was used as an endogenous control for data analysis (Mah *et al*., 2003).

Virulence assay

The local leaf maceration assay was performed using the leaves of Chinese cabbage (*B. campestris*) and African violet (*S. ionantha*) as described (Yi *et al*., 2010). For African violet, 50 μl of bacterial suspension at 10^6 CFU ml^{-1} were syringe infiltrated in the middle of each symmetric side of the same leaf. Phosphate buffer (50 mM, pH 7.4) was used to suspend the bacterial cells. Five replicate plants were used for each bacterial strain, and four leaves were inoculated in each plant. For Chinese cabbage, 10 μl of bacterial suspension at 10^7 CFU ml^{-1} were inoculated into the wounds punched with a sterile pipette on the leaves. Five leaves were used for each strain. Inoculated African violet plants or Chinese cabbage leaves were kept in growth chamber at 28°C with 100% relative humidity. To evaluate disease symptoms, APS ASSESS 1.0 software (Image Analysis Software for Plant Disease Quantification) was used to determine the leaf maceration area.

Statistical analysis

Means and standard deviations of experimental results were calculated using EXCEL (Microsoft, Redmond, WA), and the statistical analysis was performed using a two-tailed *t*-test.

Acknowledgements

This work is dedicated to Noel T. Keen. We thank Loryn Zachariasen for measurements and data analysis on Förster resonance energy transfer assay and Susu Fan for cloning and site-directed mutagenesis of $bcsA_{3937}$ of *D. dadantii*. We also thank Dr. Hemantha Kulasekara from Dr. Samuel Miller's lab for providing the pMMB67EHGent vector and derivative plasmids. This project was supported by grants from the National Science Foundation (award no. EF-0332163 to C.-H. Yang), the National Science Foundation (Grants PHY-1058470, IIP-1114305, and PHY-1126386 to V.R.), the Research Growth Initiative of the University of Wisconsin-Milwaukee to C.-H. Yang, and the National Science Foundation of China (award no. 31100947 to F. T.).

References

Aldridge, P.D., Karlinsey, J.E., Aldridge, C., Birchall, C., Thompson, D., Yagasaki, J., and Hughes, K.T. (2006) The flagellar-specific transcription factor, σ^{28}, is the Type III secretion chaperone for the flagellar-specific anti-σ^{28} factor FlgM. *Gene Dev* **20:** 2315–2326.

Alfano, J.R., and Collmer, A. (1997) The type III (Hrp) secretion pathway of plant pathogenic bacteria: trafficking harpins, Avr proteins, and death. *J Bacteriol* **179:** 5655–5662.

Antúnez-Lamas, M., Cabrera-Ordóñez, E., López-Solanilla, E., Raposo, R., Trelles-Salazar, O., Rodríguez-Moreno, A., and Rodríguez-Palenzuela, P. (2009) Role of motility and chemotaxis in the pathogenesis of *Dickeya dadantii* 3937 (ex *Erwinia chrysanthemi* 3937). *Microbiology* **155:** 434–442.

Bauer, D.W., Bogdanove, A.J., Beer, S.V., and Collmer, A. (1994) *Erwinia chrysanthemi hrp* genes and their involvement in soft rot pathogenesis and elicitation of the hypersensitive response. *Mol Plant Microbe Interact* **7:** 573–581.

Beaulieu, C., and Van Gijsegem, F. (1990) Identification of plant-inducible genes in *Erwinia chrysanthemi* 3937. *J Bacteriol* **172:** 1569–1575.

Benach, J., Swaminathan, S.S., Tamayo, R., Handelman, S.K., Folta-Stogniew, E., Ramos, J.E., *et al*. (2007) The structural basis of cyclic diguanylate signal transduction by PilZ domains. *EMBO J* **26:** 5153–5166.

Biener, G., Stoneman, M.R., Acbas, G., Holz, J.D., Orlova, M., Komarova, L., *et al*. (2013) Development and experimental testing of an optical micro-spectroscopic technique incorporating true line-scan excitation. *Int J Mol Sci* **15:** 261–276.

Breaker, R.R. (2011) Prospects for riboswitch discovery and analysis. *Mol Cell* **43:** 867–879.

Chatterjee, A., Cui, Y., Liu, Y., Dumenyo, C.K., and Chatterjee, A.K. (1995) Inactivation of *rsmA* leads to overproduction of extracellular pectinases, cellulases, and proteases in *Erwinia carotovora* subsp. *carotovora* in the absence of the starvation/cell density-sensing signal, N-(3-oxohexanoyl)-L-homoserine lactone. *Appl Environ Microbiol* **61:** 1959–1967.

Chatterjee, A., Cui, Y., and Chatterjee, A.K. (2002) Regulation of *Erwinia carotovora* $hrpL_{Ecc}$ (sigma-L_{Ecc}), which encodes an extracytoplasmic function subfamily of sigma factor required for expression of the Hrp Regulon. *Mol Plant Microbe Interact* **15:** 971–980.

Chilcott, G.S., and Hughes, K.T. (2000) Coupling of flagellar gene expression to flagellar assembly in *Salmonella enterica* Serovar *Typhimurium* and *Escherichia coli*. *Microbiol Mol Biol Rev* **64:** 694–708.

Christen, M., Christen, B., Allan, M.G., Folcher, M., Jenö, P., Grzesiek, S., and Jenal, U. (2007) DgrA is a member of a new family of cyclic diguanosine monophosphate receptors and controls flagellar motor function in *Caulobacter crescentus*. *Proc Natl Acad Sci USA* **104:** 4112–4117.

Christen, M., Kulasekara, H.D., Christen, B., Kulasekara, B.R., Hoffman, L.R., and Miller, S.I. (2010) Asymmetrical distribution of the second messenger c-di-GMP upon bacterial cell division. *Science* **328:** 1295–1297.

Claret, L., and Hughes, C. (2002) Interaction of the atypical prokaryotic transcription activator $FlhD_2C_2$ with early promoters of the flagellar gene hierarchy. *J Mol Biol* **321:** 185–199.

Collmer, A., and Keen, N.T. (1986) The role of pectic enzymes in plant pathogenesis. *Annu Rev Phytopathol* **24:** 383–409.

Cotter, P.A., and Stibitz, S. (2007) c-di-GMP-mediated regulation of virulence and biofilm formation. *Curr Opin Microbiol* **10:** 17–23.

Cui, Y., Chatterjee, A., Yang, H., and Chatterjee, A.K. (2008) Regulatory network controlling extracellular proteins in *Erwinia carotovora* subsp. *carotovora*: FlhDC, the master regulator of flagellar genes, activates *rsmB* regulatory RNA production by affecting *gacA* and *hexA* (*lrhA*) expression. *J Bacteriol* **190:** 4610–4623.

Czajkowski, R., Pérombelon, M.C., van Veen, J.A., and van der Wolf, J.M. (2011) Control of blackleg and tuber soft rot of potato caused by *Pectobacterium* and *Dickeya* species: a review. *Plant Pathol* **60:** 999–1013.

Datsenko, K.A., and Wanner, B.L. (2000) One-step inactivation of chromosomal genes in *Escherichia coli* K-12 using PCR products. *Proc Natl Acad Sci USA* **97:** 6640–6645.

Edmunds, A.C., Castiblanco, L.F., Sundin, G.W., and Waters, C.M. (2013) Cyclic di-GMP modulates the disease progression of *Erwinia amylovora*. *J Bacteriol* **195:** 2155–2165.

Erhardt, M., Namba, K., and Hughes, K.T. (2010) Bacterial nanomachines: the flagellum and type III injectisome. *Cold Spring Harb Perspect Biol* **2:** a000299.

Fang, X., and Gomelsky, M. (2010) A post-translational, c-di-GMP-dependent mechanism regulating flagellar motility. *Mol Microbiol* **76:** 1295–1305.

Frye, J., Karlinsey, J.E., Felise, H.R., Marzolf, B., Dowidar, N., McClelland, M., and Hughes, K.T. (2006) Identification of new flagellar genes of *Salmonella enterica* serovar Typhimurium. *J Bacteriol* **188:** 2233–2243.

Gonzalez, R.C., Woods, R.E., and Eddins, S.L. (2004) *Digital Image Processing Using MATLAB*. New Jersey, USA: Pearson Prentice Hall.

He, S.Y., Nomura, K., and Whittam, T.S. (2004) Type III protein secretion mechanism in mammalian and plant pathogens. *BBA-Mol Cell Res* **1694:** 181–206.

Hengge, R. (2009) Principles of c-di-GMP signalling in bacteria. *Nat Rev Microbiol* **7:** 263–273.

Herron, S.R., Benen, J.A., Scavetta, R.D., Visser, J., and Jurnak, F. (2000) Structure and function of pectic enzymes: virulence factors of plant pathogens. *Proc Natl Acad Sci USA* **97:** 8762–8769.

Hommais, F., Oger-Desfeux, C., Van Gijsegem, F., Castang, S., Ligori, S., Expert, D., *et al*. (2008) PecS is a global regulator of the symptomatic phase in the phytopathogenic bacterium *Erwinia chrysanthemi* 3937. *J Bacteriol* **190:** 7508–7522.

Hueck, C.J. (1998) Type III protein secretion systems in bacterial pathogens of animals and plants. *Microbiol Mol Biol Rev* **62:** 379–433.

Jahn, C.E., Selimi, D.A., Barak, J.D., and Charkowski, A.O. (2011) The *Dickeya dadantii* biofilm matrix consists of cellulose nanofibres, and is an emergent property dependent upon the type III secretion system and the cellulose synthesis operon. *Microbiology* **157:** 2733–2744.

Kazemi-Pour, N., Condemine, G., and Hugouvieux-Cotte-Pattat, N. (2004) The secretome of the plant pathogenic bacterium *Erwinia chrysanthemi*. *Proteomics* **4:** 3177–3186.

Kulasekara, B.R., Kamischke, C., Kulasekara, H.D., Christen, M., Wiggins, P.A., and Miller, S.I. (2013) c-di-GMP heterogeneity is generated by the chemotaxis machinery to regulate flagellar motility. *Elife* **2:** e01402.

Lee, S.H., and Galán, J.E. (2004) *Salmonella* type III secretion-associated chaperones confer secretion-pathway specificity. *Mol Microbiol* **51:** 483–495.

Leveau, J.H., and Lindow, S.E. (2001) Predictive and interpretive simulation of green fluorescent protein expression in reporter bacteria. *J Bacteriol* **183:** 6752–6762.

Li, Y., Hutchins, W., Wu, X., Liang, C., Zhang, C., Yuan, X., *et al*. (2014) Derivative of plant phenolic compound inhibits the type III secretion system of *Dickeya dadantii* via HrpX/HrpY two-component signal transduction and Rsm systems. *Mol Plant Pathol* **16:** 150–163.

Liu, X., and Matsumura, P. (1994) The FlhD/FlhC complex, a transcriptional activator of the *Escherichia coli* flagellar class II operons. *J Bacteriol* **176:** 7345–7351.

Liu, Y., Cui, Y., Mukherjee, A., and Chatterjee, A.K. (1998) Characterization of a novel RNA regulator of *Erwinia carotovora* ssp. *carotovora* that controls production of extracellular enzymes and secondary metabolites. *Mol Microbiol* **29:** 219–234.

Macnab, R.M. (1996) *Escherichia coli* and *Salmonella typhimurium*: Cellular and Molecular Biology. Neidhardt, F.C., and others (eds). Washington, DC, USA: ASM, pp. 123–145.

Mah, T.-F., Pitts, B., Pellock, B., Walker, G.C., Stewart, P.S., and O'Toole, G.A. (2003) A genetic basis for *Pseudomonas aeruginosa* biofilm antibiotic resistance. *Nature* **426:** 306–310.

Matsumoto, H., Muroi, H., Umehara, M., Yoshitake, Y., and Tsuyumu, S. (2003) Peh production, flagellum synthesis, and virulence reduced in *Erwinia carotovora* subsp. *carotovora* by mutation in a homologue of *cytR*. *Mol Plant Microbe Interact* **16:** 389–397.

Miller, W.G., Leveau, J.H., and Lindow, S.E. (2000) Improved *gfp* and *inaZ* broad-host-range promoter-probe vectors. *Mol Plant Microbe Interact* **13:** 1243–1250.

Morgan, J.L., McNamara, J.T., and Zimmer, J. (2014) Mechanism of activation of bacterial cellulose synthase by cyclic di-GMP. *Nat Struct Mol Biol* **21:** 489–496.

Mota, L.J., Sorg, I., and Cornelis, G.R. (2005) Type III secretion: the bacteria-eukaryotic cell express. *FEMS Microbiol Lett* **252:** 1–10.

Otsu, N. (1975) A threshold selection method from gray-level histograms. *Automatica* **11:** 23–27.

Pallen, M.J., Beatson, S.A., and Bailey, C.M. (2005) Bioinformatics, genomics and evolution of non-flagellar type-III secretion systems: a Darwinian perspective. *FEMS Microbiol Rev* **29:** 201–229.

Patowary, S., Alvarez-Curto, E., Xu, T.-R., Holz, J.D., Oliver, J.A., Milligan, G., and Raicu, V. (2013) The muscarinic M3 acetylcholine receptor exists as two differently sized complexes at the plasma membrane. *Biochem J* **452:** 303–312.

Paul, K., Nieto, V., Carlquist, W.C., Blair, D.F., and Harshey, R.M. (2010) The c-di-GMP binding protein YcgR controls flagellar motor direction and speed to affect chemotaxis by a 'backstop brake' mechanism. *Mol Cell* **38:** 128–139.

Paul, R., Weiser, S., Amiot, N.C., Chan, C., Schirmer, T., Giese, B., and Jenal, U. (2004) Cell cycle-dependent dynamic localization of a bacterial response regulator with a novel di-guanylate cyclase output domain. *Gene Dev* **18:** 715–727.

Peng, Q., Yang, S., Charkowski, A.O., Yap, M.-N., Steeber, D.A., Keen, N.T., and Yang, C.-H. (2006) Population behavior analysis of *dspE* and *pelD* regulation in *Erwinia chrysanthemi* 3937. *Mol Plant Microbe Interact* **19:** 451–457.

Pesavento, C., Becker, G., Sommerfeldt, N., Possling, A., Tschowri, N., Mehlis, A., and Hengge, R. (2008) Inverse regulatory coordination of motility and curli-mediated adhesion in *Escherichia coli*. *Gene Dev* **22:** 2434–2446.

Pfaffl, M.W., Horgan, G.W., and Dempfle, L. (2002) Relative expression software tool (REST©) for group-wise comparison and statistical analysis of relative expression results in real-time PCR. *Nucleic Acids Res* **30:** e36.

Prigent-Combaret, C., Zghidi-Abouzid, O., Effantin, G., Lejeune, P., Reverchon, S., and Nasser, W. (2012) The nucleoid-associated protein Fis directly modulates the synthesis of cellulose, an essential component of pellicle-biofilms in the phytopathogenic bacterium *Dickeya dadantii*. *Mol Microbiol* **86:** 172–186.

Raicu, V., and Singh, D.R. (2013) FRET spectrometry: a new tool for the determination of protein quaternary structure in living cells. *Biophys J* **105:** 1937–1945.

Raicu, V., Stoneman, M.R., Fung, R., Melnichuk, M., Jansma, D.B., Pisterzi, L.F., *et al*. (2009) Determination of supramolecular structure and spatial distribution of protein complexes in living cells. *Nat Photonics* **3:** 107–113.

Rojas, C.M., Ham, J.H., Deng, W.-L., Doyle, J.J., and Collmer, A. (2002) HecA, a member of a class of adhesins produced by diverse pathogenic bacteria, contributes to the attachment, aggregation, epidermal cell killing, and virulence phenotypes of *Erwinia chrysanthemi* EC16 on *Nicotiana clevelandii* seedlings. *Proc Natl Acad Sci USA* **99:** 13142–13147.

Roy, C., Kester, H., Visser, J., Shevchik, V., Hugouvieux-Cotte-Pattat, N., Robert-Baudouy, J., and Benen, J. (1999) Modes of action of five different endopectate lyases from *Erwinia chrysanthem*i 3937. *J Bacteriol* **181:** 3705–3709.

Römling, U. (2012) Cyclic di-GMP, an established secondary messenger still speeding up. *Environ Microbiol* **14:** 1817–1829.

Ryan, R.P., Fouhy, Y., Lucey, J.F., Crossman, L.C., Spiro, S., He, Y.-W., *et al*. (2006) Cell–cell signaling in *Xanthomonas campestris* involves an HD-GYP domain protein that functions in cyclic di-GMP turnover. *Proc Natl Acad Sci USA* **103:** 6712–6717.

Ryan, R.P., Tolker-Nielsen, T., and Dow, J.M. (2012) When the PilZ don't work: effectors for cyclic di-GMP action in bacteria. *Trends Microbiol* **20:** 235–242.

Ryjenkov, D.A., Simm, R., Römling, U., and Gomelsky, M. (2006) The PilZ domain is a receptor for the second messenger c-di-GMP: the PliZ domain protein YcgR controls motiltiy in enterobacteria. *J Biol Chem* **281:** 30310–30314.

Schirmer, T., and Jenal, U. (2009) Structural and mechanistic determinants of c-di-GMP signalling. *Nat Rev Microbiol* **7:** 724–735.

Schmidt, A.J., Ryjenkov, D.A., and Gomelsky, M. (2005) The ubiquitous protein domain EAL is a cyclic diguanylate-specific phosphodiesterase: enzymatically active and inactive EAL domains. *J Bacteriol* **187:** 4774–4781.

Solano, C., García, B., Latasa, C., Toledo-Arana, A., Zorraquino, V., Valle, J., *et al*. (2009) Genetic reductionist approach for dissecting individual roles of GGDEF proteins within the c-di-GMP signaling network in *Salmonella*. *Proc Natl Acad Sci USA* **106:** 7997–8002.

Srivastava, D., Hsieh, M.L., Khataokar, A., Neiditch, M.B., and Waters, C.M. (2013) Cyclic di-GMP inhibits *Vibrio cholerae* motility by repressing induction of transcription and inducing extracellular polysaccharide production. *Mol Microbiol* **90:** 1262–1276.

Stafford, G.P., Ogi, T., and Hughes, C. (2005) Binding and transcriptional activation of non-flagellar genes by the *Escherichia coli* flagellar master regulator $FlhD_2C_2$. *Microbiology* **151:** 1779–1788.

Tamayo, R., Tischler, A.D., and Camilli, A. (2005) The EAL domain protein VieA is a cyclic diguanylate phosphodiesterase. *J Biol Chem* **280:** 33324–33330.

Tang, X., Xiao, Y., and Zhou, J.-M. (2006) Regulation of the type III secretion system in phytopathogenic bacteria. *Mol Plant Microbe Interact* **19:** 1159–1166.

Tuckerman, J.R., Gonzalez, G., and Gilles-Gonzalez, M.-A. (2011) Cyclic di-GMP activation of polynucleotide phosphorylase signal-dependent RNA processing. *J Mol Biol* **407:** 633–639.

Wang, S., Fleming, R.T., Westbrook, E.M., Matsumura, P., and McKay, D.B. (2006) Structure of the *Escherichia coli* FlhDC complex, a prokaryotic heteromeric regulator of transcription. *J Mol Biol* **355:** 798–808.

Wei, H.-L., Chakravarthy, S., Worley, J.N., and Collmer, A. (2013) Consequences of flagellin export through the type III secretion system of *Pseudomonas syringae* reveal a major difference in the innate immune systems of mammals and the model plant *Nicotiana benthamiana*. *Cell Microbiol* **15:** 601–618.

Wei, Z.-M., and Beer, S.V. (1995) *hrpL* activates *Erwinia amylovora* hrp gene transcription and is a member of the ECF subfamily of sigma factors. *J Bacteriol* **177:** 6201–6210.

Yang, C.-H., Gavilanes-Ruiz, M., Okinaka, Y., Vedel, R., Berthuy, I., Boccara, M., *et al*. (2002) *hrp* genes of *Erwinia chrysanthemi* 3937 are important virulence factors. *Mol Plant Microbe Interact* **15:** 472–480.

Yang, S., Zhang, Q., Guo, J., Charkowski, A.O., Glick, B.R., Ibekwe, A.M., *et al*. (2007) Global effect of indole-3-acetic

acid biosynthesis on multiple virulence factors of Erwinia chrysanthemi 3937. *Appl Environ Microbiol* **73:** 1079–1088.

Yang, S., Peng, Q., San Francisco, M., Wang, Y., Zeng, Q., and Yang, C.-H. (2008a) Type III secretion system genes of *Dickeya dadantii* 3937 are induced by plant phenolic acids. *PLoS ONE* **3:** e2973.

Yang, S., Peng, Q., Zhang, Q., Yi, X., Choi, C.J., Reedy, R.M., *et al*. (2008b) Dynamic regulation of GacA in type III secretion, pectinase gene expression, pellicle formation, and pathogenicity of *Dickeya dadantii* (*Erwinia chrysanthemi* 3937). *Mol Plant Microbe Interact* **21:** 133–142.

Yap, M.-N., Yang, C.-H., Barak, J.D., Jahn, C.E., and Charkowski, A.O. (2005) The *Erwinia chrysanthemi* type III secretion system is required for multicellular behavior. *J Bacteriol* **187:** 639–648.

Yi, X., Yamazaki, A., Biddle, E., Zeng, Q., and Yang, C.H. (2010) Genetic analysis of two phosphodiesterases reveals cyclic diguanylate regulation of virulence factors in *Dickeya dadantii*. *Mol Microbiol* **77:** 787–800.

Young, G.M., Schmiel, D.H., and Miller, V.L. (1999) A new pathway for the secretion of virulence factors by bacteria: the flagellar export apparatus functions as a protein-secretion system. *Proc Natl Acad Sci USA* **96:** 6456–6461.

Zogaj, X., Nimtz, M., Rohde, M., Bokranz, W., and Römling, U. (2001) The multicellular morphotypes of *Salmonella typhimurium* and *Escherichia coli* produce cellulose as the second component of the extracellular matrix. *Mol Microbiol* **39:** 1452–1463.

Zorraquino, V., García, B., Latasa, C., Echeverz, M., Toledo-Arana, A., Valle, J., *et al*. (2013) Coordinated cyclic-di-GMP repression of *Salmonella* motility through YcgR and cellulose. *J Bacteriol* **195:** 417–428.

Supporting information

Additional Supporting Information may be found in the online version of this article at the publisher's website:

Fig. S1. Isothermal titration calorimetric analysis of c-di-GMP binding to wild-type $YcgR_{3937}$ (A) or the point mutation version $YcgR_{3937}^{R124D}$ (B). Calorimetric titration for c-di-GMP (500 μM) titrated into test proteins (50 μM) is shown. Derived values for K_d and stoichiometry (N) are shown.

Fig. S2. Swimming motility was measured in *D. dadantii*. All results are shown from one representative experiment, three independent experiments were performed and three replicates were used for each experiment. Error bars indicate standard errors of the means. Asterisks indicate statistically significant differences of the means ($P < 0.05$ by Student's *t*-test).

Fig. S3. Measurement of *D. dadantii* virulence to African violet (*Saintpaulia ionantha*). Bacterial cells of the wild-type *D. dadantii*, *flhDC* and *fliA* mutant strains and complemented strains were inoculated in the leaves of African violet. The maceration symptom was measured 2 days post-inoculation. Maceration assays were performed as described in the Experimental procedures. Error bars indicate standard errors of the means. Asterisks indicate statistically significant differences of the means ($P < 0.05$ by Student's *t*-test).

Fig. S4. Pectate lyase production and swimming motility were measured in the parental strain *D. dadantii* 3937 harbouring empty vector pCL1920, Δ*flhDC* harbouring empty pCL1920, Δ*flhDC* harbouring pCL1920-*flhDC*, Δ*flhDC* harbouring pCL1920-*ecpC* and Δ*flhDC* harbouring pCL1920-*rsmB* respectively. Assays were performed as described in the Experimental procedures. The experiments were repeated three independent times with similar results. The figure represents data from one experiment which includes three to five technical replicates. Error bars indicate standard errors of the means. Asterisks indicate statistically significant differences of the means ($P < 0.05$ by Student's *t*-test).

Table S1. Plasmid constructs used in this study.

Table S2. Primers used in this study.